TRIUMF

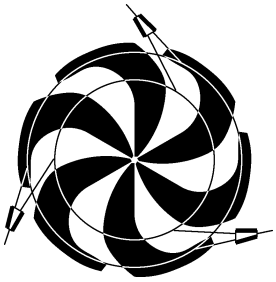

ANNUAL REPORT
SCIENTIFIC ACTIVITIES
1999

ISSN 1492-417X

CANADA'S NATIONAL LABORATORY
FOR PARTICLE AND NUCLEAR PHYSICS

OPERATED AS A JOINT VENTURE

MEMBERS:

THE UNIVERSITY OF ALBERTA
SIMON FRASER UNIVERSITY
THE UNIVERSITY OF VICTORIA
THE UNIVERSITY OF BRITISH COLUMBIA

ASSOCIATE MEMBERS:

CARLETON UNIVERSITY
THE UNIVERSITY OF MANITOBA
L'UNIVERSITÉ DE MONTRÉAL
QUEEN'S UNIVERSITY
THE UNIVERSITY OF REGINA
THE UNIVERSITY OF TORONTO

UNDER A CONTRIBUTION FROM THE
NATIONAL RESEARCH COUNCIL OF CANADA

JULY 2000

The contributions on individual experiments in this report are outlines intended to demonstrate the extent of scientific activity at TRIUMF during the past year. The outlines are not publications and often contain preliminary results not intended, or not yet ready, for publication. Material from these reports should not be reproduced or quoted without permission from the authors.

ISAC PROJECT

INTRODUCTION

This has again been a year of considerable and visible progress in ISAC. Two new target modules for the west target tank were built. The south hot cell was completed and was used to remotely replace activated targets. The remote control system for the target hall crane system was completed and used to successfully transport target modules between the target tank and the hot cell. The GPS1 (lifetime station) was moved from its temporary location to the final LEBT position. The LEBT was completed to the LTNO, the GPS1 and β-NMR stations. A yield station was added to the top of the LEBT vertical beam line. All of these beam lines were commissioned with beam. The beam dynamics properties of the ^{8}Li polarizer were successfully tested on the ion source test stand using ^{7}Li and the assembly was then installed on the LEBT in the ISAC hall. Initial beam operation to TRINAT, LTNO and GPS1 was started with a core group of operators. There has also been a great deal of effort and progress by the numerous support groups working on ISAC infrastructure. As a result key milestones were achieved on time.

Meanwhile, progress on the accelerated beams has been slightly delayed by giving priority to the completion of the new target module required for the high beam power test. Nevertheless the RFQ was completed and commissioned at full power. Beams from the offline ion source were used in Test #1 to confirm that the accelerated beam quality from the RFQ was as predicted. The MEBT is now nearly ready for Test #2 which entails sending a full energy beam from the RFQ through a carbon foil stripper and the charge selection slits onto a fast Faraday cup downstream of the second 45° dipole. Test #3 requires the MEBT spiral rebuncher, the first DTL tank, the first magnetic triplet and the split-ring buncher and is scheduled for late April, 2000. All of the DTL tanks, bunchers, magnetic triplets and HEBT dipoles have now been ordered and are being manufactured. Most of the quadrupoles for HEBT will come from the Chalk River/TASCC equipment. The overall schedule predicts that a stable accelerated beam will be ready for a high-energy experimental station by the end of 2000.

ISAC achieved three major milestones in 1999. First, operation began on July 29 with a 10 μA proton beam on a Nb target. This target yielded record intensities of ^{74}Rb. Next, on December 3, an unpolarized ^{8}Li beam (from the Nb target) with an intensity close to 10^{7} particles/sec was successfully transported with little loss to the β-NMR experimental station where the β-NMR group confirmed the lifetime of the ^{8}Li. AECB granted a licence amendment on November 26 to permit a target test with 100 μA of protons. To avoid unnecessary activation of the target, BL2A was initially commissioned without a target at 100 μA early in December. Finally, on December 17, a 100 μA proton beam was successfully used to test the thermal properties of a thick molybdenum target.

ISAC OPERATIONS

This year marked a transition between construction and operation of the ISAC facility. Beam physicists and commissioning engineers had delivered the initial beam in late 1998. The first of the ISAC Operations group were hired in April, 1999, and they provided the nucleus of support for the commissioning and initial operation of various ISAC facilities which was done throughout the year. There was still, however, heavy reliance on the physicists and engineers, and the hours of operation had to be restricted at times due to a lack of qualified Operations staff to provide continuous operation. At year end, the group was comprised of Andy Hurst as group leader, Jaroslav Welz as maintenance engineer, Mike Hauser as coordinator, Damien Gallop and Violeta Toma as operators. Three operators are to be hired in the first quarter of 2000 to bring the group to the minimum level required to satisfy continuous operation (without contingency for absences due to illness and vacation entitlements). An ISAC organizational structure defining the extent of the Operations responsibilities is also expected in the new year. These responsibilities may include various coordination and maintenance roles in the target hall, mass separator room and some areas of the experiment hall.

The basic roles of the ISAC Operations group are comparable to the other cyclotron Operation groups at TRIUMF (500 MeV Operations and the ATG).

Similar systems have been implemented for internal shift communications, operations notes and console log books, work permits and safety defeats. The fault reporting is done electronically via a Web interface and there is also an electronic log book. The major effort in the coming year will be to establish operation and service manuals and training programs for Operations staff.

Maintenance and commissioning activities have been coordinated throughout the year, with a weekly electronic distribution of maintenance schedules based on requests solicited from support groups. This has helped to smooth many of the conflicts which arise during beam operation to scheduled experiments simultaneous with on-going construction and commissioning of nearby new beam lines.

An annual report will usually provide operational

performance statistics, but these are not as relevant during commissioning periods when systems are not always fully functional. Also, the lack of operations staff in 1999 has limited the ability to maintain performance statistics. The data has been kept, but summaries are not available at this time. Nevertheless, it can be stated that all scheduled experiments received enough beam to satisfy their commissioning milestones and preliminary experiment requirements. The members of the Operations group take great pride in their contributions to the successes of the major ISAC milestones which were achieved this year and have been highlighted elsewhere in this Annual Report.

CONVENTIONAL FACILITIES AND INFRASTRUCTURES

The Infrastructure group continued to enjoy a busy and productive year. Efforts focused on the experimental hall services since beam delivery to the experimental facilities in the low energy area was a priority. Coordination work continued with the Science Division and the Accelerator group for the general arrangement of facilities on the experimental floor and the integration of the building services. This included attendance at regular progress meetings, participation in design reviews and maintaining the as-built arrangement drawings. The group continued to provide support to other ISAC groups for services design and engineering, material procurement and coordination of outside labour. Maintenance was carried out with the help of the Plant group and the electrical department. A few problems with the plant facilities were corrected. The problems discovered during the commissioning of the target hall crane were finally resolved to the satisfaction of TRIUMF. The remote controls for the crane are being implemented by TRIUMF. A much needed finer motion control was added to the experimental hall crane. All floor openings were sealed to control the airflow between various pressure zones. Other tasks completed during the year included the target assembly and the cold chemistry rooms, and the improvement of the second floor of the target maintenance building. The Design/Drafting group relocated to its new office in August. Discussion started for planning the gas handling facility and a liquid nitrogen facility and to provide waterproofing of the penthouse floor. Land and building requirements for the ISAC-II experimental program in the next five-year plan were studied.

Data and Voice Communication

The Data Communications group continued the installation of 100 base-T cables; 10 cables were added to the LE experimental area, 5 of which were terminated. A 12-strand fiber cable (450 ft in length) was pulled to the radiochemistry building to connect to the central station. The Design Office was cabled with a 100 Mbps link, and some sixty 10/100 outlets throughout the office. All conduits were traced, mapped and as-built drawings produced for the public address system. Cables were pulled and identified.

Telephone locals were added as the need arose. The major contribution was the design and installation of the telephone system for the Design Office.

Electrical Services

The expansion of the electrical distribution system and the installation of services in the experimental hall continued at a fast pace. The priority was to ensure beam delivery to the low energy experimental facilities (LTNO, GPS, yield station, β-NMR) and the commissioning of linac sub-systems (RFQ/MEBT). Controls racks and power supplies were housed on the elevated mezzanine around the perimeter of the experimental hall. Work started on the design of the DRAGON facility services and on the identification of the services required for the HEBT beam line components and the TUDA facility. Space limitations on the north mezzanine forced the relocation of some electrical services on the ground floor to make room for the HEBT power supplies and controls racks. An electrically shielded data acquisition room is planned for TUDA to minimize electrical interference and disturbances to the very sensitive detector electronics.

Major tasks completed during the year included the installation of the dc and ac power distribution, racks for beam line power supplies, controls and diagnostics, and cable tray systems for the following systems/areas:

- Low energy beam transport section to the β-NMR station. Beam optics power supplies were housed in racks overlooking LEBT on the south elevated mezzanine.
- Low energy experimental facilities (LTNO, GPS, yield station, β-NMR). The grounding and the power distribution for LTNO were engineered to accommodate the complete galvanic isolation from the rest of the world except for a safety ground point. The electrical systems for β-NMR were designed to allow operation at 60 kV bias on a raised voltage station platform. The installation of the services on the platform is scheduled for early in the year 2000.
- MEBT power supplies and controls racks were housed on the northwest mezzanine.
- DTL services included the power distribution, racks and power to 8 rf amplifiers. The part of the work on the floor will be installed during the next year.

- Conduit installation for the radiation safety monitoring system in the LE experimental area.
- Hot cell services including controls for the manipulators, turntable and lighting.
- DRAGON gas target facility services.

Other tasks completed included services to the hot cells, target assembly room, cold chemistry laboratory and the new Design Office in the target maintenance building.

The start-up time of the emergency power bus (diesel generator) was adjusted down to 12 s to satisfy a commissioning requirement of the target cooling system. The secondary cooling-loop pumps were added to the list of safety-critical loads and connected to the emergency power bus. This required upgrades in the breaker coordination of a couple of load panels. Late in July the experimental hall UPS suffered a major failure. We had to replace an expensive rectifier card and associated power supply on one of the 3 phase legs. Troubleshooting of problems in some communication cards associated with the target station exit module optics power supplies revealed that they were induced by sparks in the target ion source. A few ideas were tested in the field as to the best way to reduce the inductive coupling between the two areas. Adding a low-pass filter at the power supply end of the high voltage cables for the steerers immediately following the surface source did the job.

Mechanical Services

The ISAC mechanical project work was aimed toward beam production and included the completion and commissioning of the nuclear exhaust zoning system and the high active cooling water system for the target station. In the case of the exhaust system it entailed final connections to the target caves and hot cells and installation of related HEPA filters, control systems, dampers, and alarms. Gauges and labels for the inter-zone doorways were installed to allow personnel to ascertain correct zoning operation before entering. Upon mechanical completion, the system was balanced to obtain the prescribed zone differential pressures. The system responded exactly as intended with increasing depressions provided as one moves from the outside world into three sequential zones. The high active water cooling system was completed and commissioned for use in RIB production. Various scenarios of filling, venting, operation, mechanical and electrical failure modes for ensured backup pump operation were demonstrated. At completion, detailed operating instructions were issued and reviewed with Operations staff. Other work included mechanical services to various areas of ISAC: water, gas and exhaust for the target assembly room fume hoods; completion of HVAC system for the new Design Office; completion of TRINAT clean room HVAC and cooling water; and compressed air into the remote handling room. The largest effort was in the experimental hall where temperature regulated and non-regulated water, compressed air, and vacuum roughing and exhaust lines were run and connected for the beam lines LEBT and MEBT and for the experimental facilities LTNO, GPS and β-NMR, and MEBT power supplies. Work started on the DTL and DRAGON services. Design work and orders were completed for the TRINAT floor cooling water return pressure control system. Engineering assistance was provided to various areas including: orifice re-sizing for Chalk River flow switches; flow rate calculations for drift tube spiral and MEBT buncher, and rough modelling of thermal expansion of the DTL end plates. Cost estimates were provided for the proposed target hall washroom, and ISAC-II.

SAFETY AND RADIATION CONTROL

Licensing

Early in 1999 a submission was made to the Atomic Energy Control Board (AECB) of Canada for a licence amendment to proceed to operate ISAC with a proton beam current of up to 10 μA on any target up to $Z = 82$. The submission was made on the basis that a number of support systems would be ready before beam production at these levels. A licence amendment was granted in time to meet the tight schedule for commissioning and radioactive ion beam production for the scientific program. The ISAC Safety Committee monitored the progress in completing all conditions set by the licence amendment.

In mid-1999 preparation of a submission was started to request permission to perform a test of a high-power Mo target. The request was finally submitted in late fall and a licence amendment was obtained several weeks before the test was scheduled to take place.

Access Control and Radiation Monitoring

The access control system for the ISAC target maintenance hall (ITMH) was completed in 1999. This system is unique at TRIUMF in that it does not interact with the accelerator access control system. Its sole function is to exclude personnel during the remote operation of the crane in the ITMH. The system interacts with the crane controls so as to prevent remote operation whenever the ITMH is not in a secured state. There is a provision for a 'test mode' which allows Remote Handling group personnel to have someone stationed in the hall during commissioning of the system if this is acknowledged by both the person in the hall and the remote crane driver.

A new radiation monitoring system for the radioactive ion beam lines was commissioned in 1999. This system has similar functionality to the existing TRIUMF radiation monitoring system but is based on VME hardware and EPICS software. The system generates local audible and visual alarms when excessive ion beam losses are detected. It is interfaced to the ISAC safety system which shuts off the ion beam when a trip level is exceeded. By year end the work had progressed to the point where these systems were functional with monitors installed along the LEBT from TRINAT to the LTNO. A display and alarm were installed in the ISAC control room and the data may be displayed on an X-terminal anywhere on the local network.

Commissioning

Commissioning largely took the form of parasitic measurements made during beam production for the scientific program. There were several highly successful runs on Nb targets at the 10 μA level. These showed that the loose radioactivity generated by the target was largely confined within the primary vacuum system and concentrated on the extraction electrodes. Several radionuclides demonstrated high mobility, among them, not unexpectedly, the Br isotopes, but also ^{75}Se. The latter forms a highly volatile hydride and may be transported through the vacuum system in this form. There was some streaming of neutrons observed through the pre-separator cave and up into the TRINAT experimental area. This emphasized the need for additional shielding to be installed between the target vessel and the pre-separator magnet.

A set of useful measurements was made during the 100 μA tests in early December. A trace of the beam current on target during the test is shown in Fig. 119.

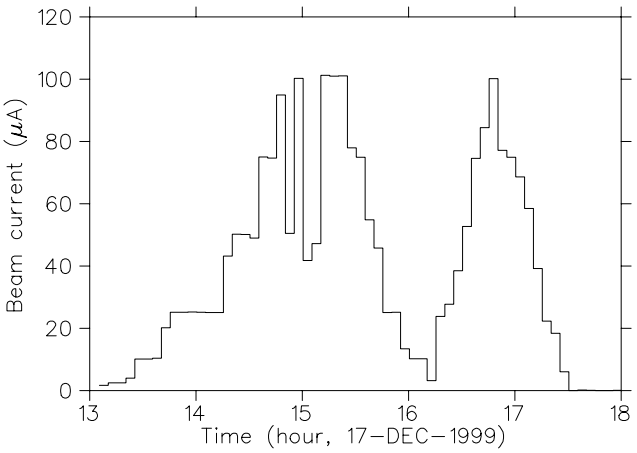

Fig. 119. Proton beam current in beam line 2A during the 100 μA test on a Mo target. There were two cycles of increasing and then decreasing the beam current in steps of 25 μA, with a brief interruption during the first cycle.

Most of the radiological parameters where within range of the estimates. The neutron fields directly above the target station appear significantly higher than estimated, although detailed comparison will require a measurement of the neutron spectrum at this location.

ISAC-I EXPERIMENTAL FACILITIES

The ISAC experimental facilities became a focus of attention at ISAC in 1999. In particular, the low energy area has seen a lot of activity (in several meanings of the word!) with the consolidation of the initial beam delivery systems and the commissioning of the new facilities (the low temperature nuclear orientation facility (LTNO) and the β-NMR complex). In the high energy area, considerable progress was made on the DRAGON facility which moved from the conceptual stage to the design, fabrication and initial installation stage, and a major award from the U.K. funding agency has made TUDA (the TRIUMF-U.K. detector array) a reality.

To summarize activities in the low energy area, we have moved from the temporary set-up, which allowed the first experiments to receive ISAC beams in November–December, 1998, to a permanent installation for TRINAT, the general purpose station (GPS) and LTNO, with a reference yield station at the exit of the vertical section of the low energy beam transport. We also installed the second main beam line which accommodates the polarizer system to produce $^{8}\overrightarrow{\text{Li}}$ and the ultra-high vacuum station for the condensed matter program using β-NMR techniques. With the commissioning of all these systems and the beginning of substantial data-taking for two programs (the $\beta - \nu$ correlation measurement in $^{38\text{m}}$K $0^+ \rightarrow 0^+$ transitions at TRINAT and the very precise lifetime measurement of $^{38\text{m}}$K, ^{37}K and ^{74}Rb beta decaying nuclei, see Expts. 715 and 823 in the Nuclear and Atomic Physics section), the low energy area now has four major scientific set-ups. Further demands for experiments are being considered as the 8π spectrometer will be repatriated from LBL later in 2000 and several other groups would like to develop ion traps, a spin manipulation apparatus and a dilution refrigerator station.

In the high energy area, two major (multi million dollar) facilities have been under construction for the nuclear astrophysics program.

The DRAGON spectrometer concept was finalized and several components were delivered this year: the windowless gas target built at the University of Alberta, as well as several sextupole and quadrupole magnets. A review of the electrostatic dipoles took place in May and construction of their power supplies and titanium electrodes was launched. DRAGON's final configuration and associated services routing were adopted and installation of components and services started.

The configuration of two of the high energy beam lines was frozen and the location and requirements for TUDA were specified. An electrically shielded room will be constructed to house the sensitive electronics for the silicon detector arrays. With the milestone of the first high energy beam to be delivered by Christmas, 2000, the focus of attention will shift in 2000 to the high energy experimental facilities.

TARGET HALL

Civil construction of the target hall was completed in 1998 and a complete description of the hall and the construction activities can be found in the 1998 Annual Report. At the end of the last reporting period the west target station (ITW) had been completed to the point where the milestone of producing radioactive beam and transporting it to the experimental hall was achieved. The goal of running a test of 100 μA protons in December, as well as several runs at 10 μA during the year meant that equipment dealing with the transportation of modules, the handling of radioactive components, i.e., targets and containment box components, storage of modules and radioactive components, and completion of shielding, had to be addressed and brought forward towards completion. This has been the main thrust of activity during this reporting period. As a result, the following goals have been achieved and will be detailed later in this report.

1. Shielding upgraded to allow the 1999 planned runs.
2. Completion of the remotely operable control system for the target hall crane.
3. Establishment of a video system to allow the remote handling and transportation of modules.
4. Completion and installation of storage silos in the target hall storage pit.
5. Installation of an interim warm cell prior to the completion of the south hot cells.

This has allowed the planned 10 μA runs to be successfully achieved and later in the year the 100 μA test was run with very few problems.

Shielding

Basic shielding had been completed prior to 1999 allowing runs of 1 μA of protons on target in order to achieve the production of radioactive ion beam and transport to the experimental hall. These early runs indicated some minor deficiencies in the shielding around the target station, i.e., high active water package, and in the pre-separator magnet area. To this end special shielding was made to surround the high active water package, and even more specialized shielding is required to complete this area. In the pre-separator magnet area, shielding was installed at the exit face of the target vacuum tank to try to reduce radiation levels at the pre-separator magnet and at diagnostic station DBO where future maintenance will be required. In order to properly address this problem it has been decided to redesign the zones between the target station vacuum tanks and the pre-separator magnet (zone 5B), to consolidate the equipment allowing insertion of additional shielding to fill the voids. This work will be executed in 2000. It is also planned to fill the void between the target tanks and the adjacent shield wall with steel plates to reduce vertical neutron streaming, as well as reducing air activation.

When the east target tank was installed it was found that radiation levels were too high in and around this area due to the fact that there are no modules and the extra shielding that was there had been removed. To solve this problem two shield plugs were made to simulate the modules but to sit on the floor of the tank. These special plugs can be utilized in other locations, as required, during maintenance. Other minor refinements in shielding were also carried out throughout the target hall area.

Target Stations

The west target station (ITW) has been operational since late 1998, and little has altered since that time other than shielding additions mentioned previously and other additions and alterations related to controls and safety. A high active plastic cooling line burst during a site power interruption. This was a result of the active cooling system pumps (which cool the high active water in a heat exchanger) not being on stand-by power, thus allowing the high active water to overheat due to pumping energy. This situation has since been rectified.

Conditions in the module access area are congested due to the amount of equipment, electrical power and control cables, high voltage terminations, and safety cage, water and vacuum lines, etc. This situation is unavoidable but rearrangement, consolidation and general housekeeping must be implemented in the near future.

The east target tank was installed in the ITE target station. Previous to this the opening between the ITE and pre-separator magnet had been plugged with concrete stacked blocks and the east target tank had been used in the storage area to vacuum leak check modules. Installation of the east tank involved the final alignment procedure, and the installation of the peripheral plate shielding between the tank and the pit wall and therefore tank removal will not be necessary in future. Since no modules were available for installation into the east tank, radiation shielding was inadequate when ITW was running. As mentioned in

the above section, two special shield blocks were constructed to fit exit 1 and 2 locations and provide the necessary shielding.

Target Modules

Two new target modules were scheduled for construction during the year. Based on information obtained during the initial commissioning and brief running period of TM1, it was decided that certain aspects of that design be modified. Access to the vertical service duct required improvement and the existing containment box was not user-friendly from a hot cell point of view, hence it was completely redesigned. One of these new modules was scheduled to carry an ECR ion source, hence more conductors were required in the service duct and, as well, a wave guide had to be accommodated in the shielding. Many other improvements were also incorporated to simplify the design and reduce cost.

The first new target module was scheduled to house the special 100 μA target for testing in December. The purpose of this test was to compare experimentally measured target temperatures with those predicted by finite element analysis. To achieve this, a special target was constructed by the Amparo Corporation requesting the experiment. The target was a stack of molybdenum foils diffusion bonded together (see Expt. 839 Safety Report for details). The only services required were water cooling and thermocouple diagnostics. As such the module (TM2) housing this target had an empty service duct and the water lines and thermocouple wires were run up the pumping duct in a temporary fashion which could be easily removed after the test. This module is to be refurbished as a surface ion source module after the test. The module was completed and ready for testing in early December, and 100 μA of proton beam was achieved on December 17.

Construction of TM3 paralleled TM2 up to a point and was then left to concentrate on completion of TM2. TM3 is approximately 50% complete and will be completed during 2000 to be ready for installation of an ECR source later in the year, ready for testing in early 2001.

The original target module TM1 will be used for tests throughout 2000.

REMOTE HANDLING GROUP

The revised design shielding plugs, containment boxes and service ducts for the new target modules #2 and #3 were assembled in the ISAC experimental hall. Target module #2 was adapted during construction to support the unique 100 μA, beam-heated Mo target used successfully for a thermal heat transfer experiment. The target hall crane is now fully operable in remote mode, complete with all safety interlocks, from the ISAC Remote Handling control room. Improved CCTV viewing, position feedbacks and assembly of a permanent control console are under way. To date the ITW target module has been successfully moved, following all defined fully remote procedures, between the west target station, hot cell and warm cell facilities five separate times. Both target module #2, complete with the 100 μA experimental target, and the ITW beam dump module have also been transferred from the ITW station to interim storage shielded silos within the target hall. Target module #1, as well as the original CaO target assembly, were aligned and confirmed in the target hall alignment frame using the procedures developed for future remote component alignment. Required new jigs were designed and built for alignment of the experimental thermal heat transfer 100 μA Mo target. The target assembly was instrument aligned in the lab, and a unique target mounting plate aligned on the new target module #2 in the alignment frame. The new Nb target was jig-aligned for installation.

Shielding and air-barrier sealing between the target hall east/west target stations and the pre-separator area were completed and installed. A hinged removable hatch was designed and built for the target hall access to the hot cell service aisle below. The south hot cell has been built and is being fully integrated into operation. Well defined operational procedures, as well as new jigs and tooling for target exchange and servicing, are being developed as the opportunities present themselves. The original CaO and the new Nb surface source production targets were both successfully removed and/or replaced in the hot cell.

Prior to the high energy 100 μA beam tests, the initial rubber seals installed on the water cooled proton beam window upstream of the ISAC ITW vacuum tank on beam line 2A were replaced with metal Helicoflex, aluminum delta seals. A design revision for the beam line section between the vacuum tanks and the pre-separator magnet was begun. This will provide for improved shielding, both steel and concrete, as well as a more permanent installation of a beam line monitor at 5B. This monitor was originally installed as a temporary diagnostics device, but has proved itself invaluable to RIB tuning. The vacuum turbo-pump presently located at this area has been deemed unnecessary and will be eliminated in the new design.

ION SOURCE TEST STAND

A new version of a TRIUMF built ECR source was tested on the ISAC ion source test stand to evaluate plasma and beam characteristics in preparation for its use at the ISAC facility. In the second half of 1999 a surface ion source was installed in the ion source test

stand to deliver stable $^7Li^+$ ions to evaluate the performance of the Na and He cells which are an integral part of the polarized $^8Li^+$ beam facility at ISAC.

Microwave Ion Source Studies

An ECR ion source with a single mode resonator at 2.45 GHz was developed to produce, with high efficiency, single-charged ion beams from the gaseous radioactive elements created in the proton target of the ISAC facility.

The target-source configuration is made such that short half-life radioactive elements can be ionized and extracted with minimum decay losses. The ECR source will also be used to produce stable ion beams for the tuning of the beam transport system and, if required, for the testing of the instrumentation used in the low and high energy experiments of ISAC.

The transient time and the overall beam efficiency were studied, as they are the most critical parameters in the field of radioactive ion production. The transient time was measured using an ultrafast piezoelectric gas valve, which could be operated at a frequency of up to 2 kHz. A unique feature of this source is that the plasma chamber, consisting of a quartz tube mounted inside the resonant cavity, is considerably smaller ($\sim$170 times) than the size of the cavity itself. This leads to a decrease in the transit time of the ions towards the extraction region. Quartz tubes of various diameters (5 to 20 mm) and 80 mm long were tested. The effect of the length of the transfer tube, that links the production target with the quartz plasma chamber, on the transient time was also studied.

The total transient time of the ion source system was found to be 40 ms for the 15 mm diameter plasma chamber. This result indicates that this ion source can be used to ionize and accelerate radioactive ions with half-life higher than 100 ms without significant decay losses. Source efficiency was also estimated. This source can ionize difficult gases such as neon with reasonable ionization efficiencies (12%).

Polarized Li Beam Development

A transport line for polarized beams is being built in the LEBT section of ISAC, initially for the ^{8}Li β-NMR program in condensed matter physics. High nuclear polarization of neutral alkali-metal atoms can be produced by direct collinear optical pumping of the beam with laser light, since the ground state of these atoms can be excited with visible or near infra-red wavelengths where tunable lasers exist. This has been used extensively by Neugart *et al.* at ISOLDE to measure magnetic and quadrupole moments of unstable nuclei. A novel feature at ISAC is that the polarized beam is re-ionized in a helium gas target, allowing it to be deflected to several experimental stations and independently varied in energy over the range 0.1 keV to 90 keV at the target. No published data exist on the yield of Li^+ from a helium target, but we have shown that it is high, as expected. Helium gives the best yield of any target gas because of its very high ionization potential. In addition, the beam emittance growth due to elastic scattering on He is lower than on the heavier noble gases. The disadvantage of He is that it produces a large load on the vacuum pumping system, especially in an unpulsed beam.

The existing ion source test stand was used as a source of $^7Li^+$ at energies near 25 keV, to test out these ideas and develop the apparatus before installation in the ISAC hall. The Li test apparatus, added to the end of the source, consisted of a sodium vapour neutralizer cell, a 1.7 m long drift region, the He gas re-ionizer cell, and focusing, steering and diagnostic elements.

The basic design of the Na neutralizer cell was first developed for the KEK polarized H^- source upgrade performed at TRIUMF, for use at RHIC. The Na cell built for the ISAC polarized beam is a 19 mm aperture recycling jet target that is very clean, compact and easy to bias electrically.

The He gas target has a T-tube configuration. The He gas is cooled to 12 K by a cryogenerator, before entering the centre of a cooled 10 mm internal diameter, 20 cm long copper tube open at both ends. Thermal compensation on the target support limits the measured vertical motion of the target centre to less than 100 μm when it is cooled from room temperature to 12 K. The horizontal motion is much less. This allows alignment to be performed at room temperature. The total length of the He cell is 50 cm, including two differential pumping ports. For a given target thickness, cooling the He to 12 K from room temperature reduces the required gas flow by a factor of 5.

Transmission of the 8 π mm mrad emittance (86% contour) $^7Li^+$ beam through the empty targets was virtually 100%. The yield of Li^0 from the Na cell was more than 90%, whereas the yield of the undesired Li^- was only 0.3%. The overall system efficiency for production of re-ionized (and potentially polarized) Li^+ was 63% at the optimum He flow rate of 1.2 sccm (uncalibrated). The system efficiency appeared to be not sensitive to beam energy in the range 20–29 keV, although those measurements need to be repeated. The vacuum pressure in the He chamber was below 10^{-5} torr at the optimum He flow.

The emittance increase of the Li^+ beam was found to depend linearly on He flow rate, as expected. At the He flow rate corresponding to the maximum Li^+ yield, the emittance was 18 π mm mrad (86% contour). With the Na cell on, it was not possible to measure re-ionized

Li^+ down to zero He flow rates. It was observed, however, that the emittance extrapolated to zero flow is the same as with no Na, i.e. the Na does not increase the emittance of the incident Li^+ beam. The emittance of the re-ionized Li^+ beam is well within the acceptance of the beam optics in ISAC.

In October and November, a large fraction of the polarized Li test stand was moved to the ISAC experimental floor and integrated with the β-NMR beam line. Unpolarized $^8Li^+$ beam was successfully guided to the β-NMR experimental apparatus in December, as described elsewhere in this Annual Report.

Producing polarized ^{8}Li requires a laser system to optically pump the beam. By modifying the internal optics of one of the I4 polarized source Ti:sapphire broadband lasers, stable laser power of 0.5 W could be achieved at 673 nm, near the extreme short wavelength limit of the Ti:sapphire crystal. The resonance wavelength of Li is 671 nm, but the Doppler shift due to the velocity of the beam bridges the gap. Ti:sapphire lasers are much more convenient to use than the dye laser alternative. The possibility of using a diode laser was also investigated, but there is no commercial support for the type of laser required. A home for the lasers was established on the mezzanine level, sharing a room with the existing TRINAT facility. The general layout was agreed on and holes drilled in the ceiling up to the main experimental level, to allow transport of the laser beam to the ^{8}Li beam line. We plan to use Ar and Ti:sapphire lasers borrowed from I4.

ISAC TARGETS

During early 1999, ISAC continued to provide ^{37}K and ^{38m}K beams to the TRINAT facility and Expt. 823 (precision lifetime measurements) using two CaO targets running at the 1 μA proton current level.

In July, a target consisting of 519 0.025 mm thick niobium foils with a total thickness of 11.1 g Nb/cm^2 was installed and operated at the 1 μA proton current level. On July 27 the proton current on target was increased to 3 μA and on July 28 to the full 10 μA currently allowed by the ISAC operating licence. The Nb #1 target continued to operate at the 10 μA proton current level until the beginning of the cyclotron shutdown period on August 22 and was subsequently used (without proton beam) for ISAC mass separator commissioning until October 15. The target received $\sim$3,386 μAh of beam for a total integrated dose of $\sim 7.6\times10^{19}$ protons. The target provided record yields of ^{74}Rb to Expt. 823 and beams of ^{75}Rb and ^{79}Rb to Expt. 828/LTNO.

A second niobium foil target (537 foils, 11.5 g Nb/cm^2) was installed and operated at the 10 μA proton current level during the period November 7 to December 6. This target continued to deliver ^{74}Rb to Expt. 823, ^{79}Rb to Expt. 828/LTNO, and was also used to provide beams of ^{74}Rb, ^{78}Rb and ^{80}Rb to TRINAT for exploratory trapping studies for future experiments. Both ^{78}Rb and ^{80}Rb were successfully trapped. At the end of the operating period, the target was used to deliver a beam of ^{8}Li ($\sim 1\times10^7$/s) to the ISAC β-NMR station for commissioning of the beam transport and detector systems.

Prior to the start of the July running period, the ISAC yield measurement station and tape transport system was commissioned and was subsequently used to determine isotope yields from the Nb targets by both β- and γ-counting. Yields from the Nb #1 and Nb #2 foil targets (normalized to 1 μA p^+) are given in Table XV. Actual yields were an order of magnitude greater.

Table XV. Normalized niobium target yields.

Nuclide	Half-life	Normalized yield (nuclei/s/μA)	
		Nb #1 11.1 g/cm^2	Nb #2 11.5 g/cm^2
^{8}Li	840 ms	$\sim 1 \times 10^6$	1.4×10^6
^{9}Li	177 ms	$\sim 8 \times 10^4$	8.3×10^4
^{37}K	1.23 s	7.6×10^2	
^{38m}K	924 ms	4.4×10^3	
^{63}Ga	32.4 s		1.1×10^3
^{64}Ga	2.63 m		4.5×10^4
^{74}Ga	8.12 m		3.6×10^4
^{74}Rb	65 ms	4.4×10^2	3.7×10^2
^{75}Rb	19 s	1.5×10^4	2.8×10^4
^{76}Rb	36.8 s	1.7×10^6	
^{77}Rb	3.9 m	2.2×10^7	
^{78g}Rb	17.7 m	7.0×10^7	
^{78m}Rb	5.7 m	4.2×10^8	
^{79}Rb	23 m	4.6×10^8	
^{80}Rb	30 s	1.8×10^9	
^{81g}Rb	4.57 h	3.4×10^9	
^{82g}Rb	1.3 m	2.0×10^8	
^{82m}Rb	6.48 h	2.3×10^9	
^{84m}Rb	20.5 m	5.8×10^8	
^{86m}Rb	1.02 m	3.5×10^7	
^{88}Rb	17.8 m	1.6×10^6	
^{89}Rb	15.2 m	1.3×10^5	
^{89m}Y	15.7 s	8.8×10^5	

100 μA Target Test

In collaboration with a group from Amparo Corporation, ISAC was used to thermally test a target designed to operate with a 100 μA 500 MeV proton beam. Many molybdenum foils and spacers (i.e., a foil with a hole at the beam location) were diffusion bonded and machined to form a target which was predicted from a

computer model to yield a useful, uniform temperature over the target at a proton current of 100 μA. The target was fitted with numerous thermocouples to confirm the temperature predictions and a proton beam profile monitor, just in front of the target, to confirm the beam density and position. The proton current was cycled between 0 and 100 μA several times. The target and the profile monitor survived the test and the data is now being analyzed to account for the observed beam profile. Initial estimates at 100 μA indicate that the calculations correctly predict the measured temperatures. Approximately 200 μAh of protons were provided for the 100 μA test. The prompt radiation in the target hall and outside the building was essentially as estimated. The test confirms that 100 μA operation at ISAC on properly chosen targets is practical.

Experiment 839
Thermal test of prototype high power ISAC target
(W.L. Talbert, Amparo Corporation)

The purpose of this experiment was to test an engineered design of a prototype test target placed in the ISAC beam line, and irradiated by the TRIUMF proton beam with intensities ranging up to 100 μA. The experiment was a thermal test only; that is, the target was heavily instrumented with thermocouple arrays to record the target temperature profiles under various conditions of heating by the proton beam and no attempt was made to extract radioactive species into the ISAC facility.

The 15 cm long prototype target was fabricated from nearly 1,200 foils of 5 mm thick molybdenum that were diffusion bonded together and electrical discharge machined to a specified design shape. This shape was developed using appropriate computer analytical approaches to predict the energy deposition profile in the target induced by the beam and the thermal behaviour of the target when cooled by circulating water at the target periphery.

The goal of the target design was to provide nearly constant temperature at the centre of the 0.95 cm radius target material. A design goal of 1,700°C was chosen for the target material, molybdenum. The design target density was varied along the target, increasing along the length to make the linear energy deposition profile approximately constant by compensating with target mass for beam fluence reduction through the target. In fabrication of the target, spacer foils (similar to target foils, with a 0.95 cm radius hole) were interspersed with target foils to result in the specified target density profile, which varied in three steps from 0.415 of solid density at the entrance end, to 0.450 of solid density in the middle, to 0.500 of solid density at the exit end of the target. The target volume was incorporated into the solid (diffusion bonded) target body that was shaped to provide cooling to the target. The target shaping that resulted from thermal analysis incorporated two longitudinal fins to which the cooling lines were attached, with each fin having a machined thermal constriction with a widening taper along the target length.

The target was mounted on an ISAC target module in early December and inserted into the ISAC beam line on December 15, after a "no-target" tuning of the ISAC beam line up to 100 μA current. Instrumentation was connected to the thermocouple leads, and to a beam profile diagnostic harp stack mounted at the entrance to the target. A photograph of the target as installed is shown in Fig. 120.

The experiment was performed on December 17, with the incident beam current varied from zero to 100 μA, back down to 10 μA, and cycled again. The beam delivery was quite stable, and the target required only about 10 minutes to reach thermal equilibrium. The target turned out to be robust, as evidenced by the return of thermal equilibrium (with the same temperatures) even after momentary interruptions of the TRIUMF beam at maximum current. Sixteen high-temperature thermocouples were employed to monitor the target temperature profiles, and seven thermocouples monitored the cooling water temperatures. All the thermocouples performed flawlessly, and fluctuations in the temperature readings were well below expectations, a tribute to those at TRIUMF who provided the specialized data acquisition system. Surprisingly, the beam profile harp monitor wires survived throughout

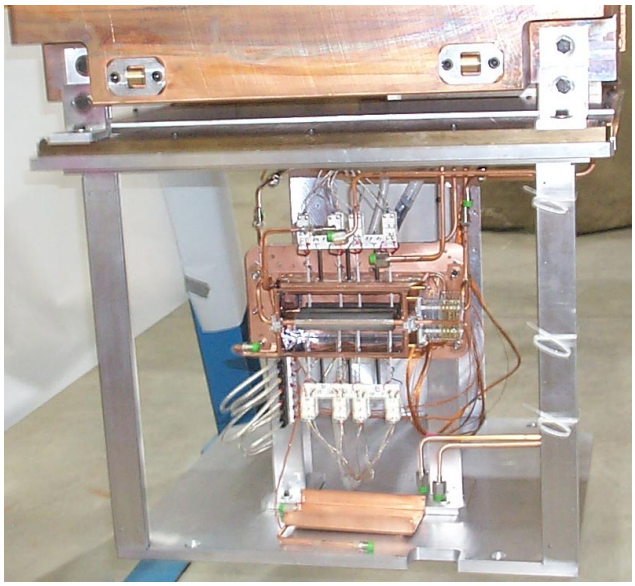

Fig. 120. Prototype target mounted on the ISAC target module. The thermocouple array is apparent in the picture.

the experiment – they were expected to burn out at currents above about 30 μA.

The resulting temperature profiles didn't correspond to the previously predicted profiles for the designed target, for the simple reason that it was discovered shortly before installation that the final electrical discharge machining of the target had been performed with the target oriented backwards. This discovery came too late to correct before performing the experiment. It was intended that the target density increase with the target axial distance; the actual target had the more dense target material at the entrance and the target density decreased with the target axial distance. This reversal in target density profile had profound effects on the observed temperature profiles, and made essential a new analysis of the target energy deposition profile and thermal behaviour. In a perverse way, this mistaken target orientation provides an even more sensitive test of the numerical approaches, because the temperatures are less intuitively predictable than for the designed configuration.

The resulting temperature profiles for the (redundant) two sets of emplaced thermocouples are shown in Figs. 121 and 122, where the new thermal analysis predictions are illustrated by smooth lines at each current, and the thermocouple temperatures are indicated as graphical symbols at 1, 6, 9 and 14 cm axial distance.

The agreement is not perfect, but the deviation is generally less than 10%, even at beam currents of 50 and 75 μA, where it is not understood why at these intermediate currents the target was apparently heated more than predicted.

During the experiment, excursions in the target module vacuum were observed for the initial increments of the TRIUMF beam current. At a current of 100 μA, the excursion was particularly prominent, but not sustained. The new thermal analysis indicates an axis temperature maximum of nearly 2000°C, for which the vapour pressure of the molybdenum target material is above 10^{-5} torr. However, these excursions are probably explained by outgassing of the target material, which was unavoidably immersed in a bath during electrical discharge machining of the assembly.

Preliminarily, the results of the experiment confirm that it is possible to use appropriate computer analysis to develop reasonable target designs for producing radioactive ion beams under conditions of high power beam heating. Temperature profiles in a developed target design would seem to be predicted to within 10%, and this validation of the numerical design approach leads the way to reliable design of actual high power targets for production of intense radioactive ion beams without embarking on an expensive empirical target development program that would demand a high commitment of scarce resources.

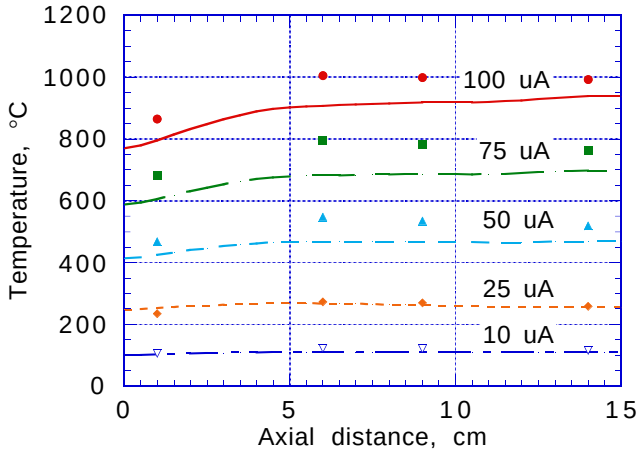

Fig. 121. Temperatures recorded by the thermocouples mounted within the cooling fins of the target, with predicted temperature profiles.

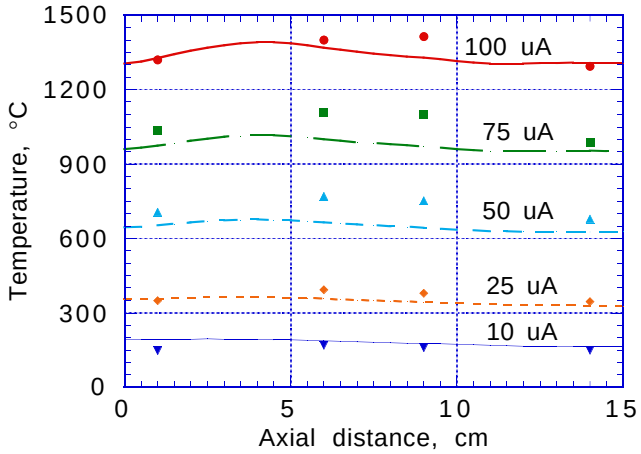

Fig. 122. Temperatures recorded by the thermocouples mounted within the target body, just outside the target volume (by 3 mm), with predicted temperature profiles.

This experiment constituted the first ever exposure of a target capable of producing radioactive ion beams to a high energy proton beam of intensity up to 100 μA, and is a landmark event leading to the eventual routine use of high power targets at ISAC.

BEAM LINE 2A

Beam line 2A transported beam to the ISAC west target station throughout the year for production of radioactive ion beams. The nominal beam current was 1 to 10 μA at 500 MeV for routine delivery depending on the target yields and experiment requirements. At year end, two separate tests were done at 100 μA: one to the beam line 2A dump with no target in place, and subsequently one to a development target provided by Amparo. These tests proved the beam line and dump

to be capable of operation at the designed beam intensity of 100 μA. Extensive radiation surveys were done during these tests and are reported elsewhere.

During the routine operation at up to 10 μA, the beam tune was mostly as predicted but at times included some unwanted components arising from various beam conditions at extraction such as the quality of the circulating beam, the type of extraction foil in use and the split ratio with respect to other beam lines. Occasionally these conditions resulted in excessive energy spread in the extracted beam, with associated losses causing trips from the radiation monitors which had been set to their most sensitive gain. More cyclotron development studies are required to understand these subtle interactions and to develop tuning techniques to minimize the effects.

MASS SEPARATOR

The first radioactive ion beam from ISAC was delivered to TRINAT in November, 1998. April, 1999 marked the beginning of ISAC operation for experiments. Beams of ^{37,38m}K and ^{74,75,79}Rb were produced for several experiments: precise half-life measurements of ^{37}K, ^{38m}K and ^{74}Rb; $\beta-\nu$ correlation in the decay of ^{38m}K using the TRINAT optical atom trap; ^{79}Rb to commission the LTNO system; plus ^{8}Li to commission the β-NMR facility.

As for the target/ion source assembly, the optic devices following the ion source are suspended at the bottom of shielding plugs. A quadrupole triplet followed by a quadrupole doublet prepares a parallel beam to the pre-separator magnet. The role of the pre-separator is to act as a cleaning stage in order to limit the contamination in the rest of the mass separator. Preliminary mass selection is achieved using a $\pm$ 60° pre-separator magnet. The pre-separator is followed by three matching sections that allow enough flexibility to match the beam in order to obtain the same mass dispersion from either target station. The mass separator magnet is the former Chalk River dipole, which became available after the laboratory shut down in 1997. The mass separator magnet including the entrance and exit matching sections are on a high voltage platform in order to allow reduction of the cross contamination and ease the magnet tuning.

The ion optics calculations were performed using the computer code GIOS. The mass separator will handle beams from mass 6 to 238 u, and source extraction voltages between 12 and 60 kV. Table XVI gives a list of the parameters for the mass separator.

The mass separator magnet is equipped with α and β coils. The α coil corrects for the magnet index and the β coil adjusts the second order correction introduced by the pole face curvature.

Table XVI. Parameters of ISAC mass separator system.

Pre-separator stage	
Deflection radius R_B	500 mm
Deflection angle θ_B	$\pm$ 60°
Air gap	70 mm
n	0.0
Mass separator stage	
Deflection radius R_B	1,000 mm
Deflection angle θ_B	135°
Air gap	100 mm
n	0.0

During the year only five days were available to test the mass separator optics. During this period we checked the quadrupole wiring and found some errors in the voltage scaling. After correction, the beam optics were in good agreement with the calculations. The beam emittance from a hot surface ion source was measured. The emittance rig uses two small slits, 50 μm wide with a $\pm$ 10 kV deflector between the slits. The emittance rig moves across the beam while the deflector scans the angular distribution of the beam going through the first slit. We were able to reconstruct the beam optics as predicted by GIOS. We were able to measure the effects of the α and β coils on the beam emittance. A third order correction, using an octupole, was also measured.

Next year it is planned to install a high voltage power supply on the high voltage platform. This will permit rejection of the cross contamination, which comes from ions of different mass in the beam having the same momentum due to collisions with the residual gas, for example. After acceleration, these ions will have a different energy and momentum and, consequently, a mass separation becomes possible.

LEBT

3-Position Switch

A new element has been designed. Its purpose is to allow fast switching of the low energy beam between different ports, and also to allow simultaneous injection of an on-axis laser beam without providing a (field-perturbing) hole in the electrostatic dipole outer electrode. It is similar to switches in use at CERN-ISOLDE, but differs in that the bend electrodes are spherical. The device which deflects the beam into benders of opposite sign (or the undeflected straight-through direction) is a 9° parallel plate deflector. (The spherical electrodes are 36° deflectors for a total of 45°.) This deflector has been treated theoretically and added to the beam optics code. The focal length in the bend direction is twice the effective length divided by the square of the deflection angle. The lowest order aberration is third order and is proportional to

the square of the quotient of the deflection angle and length, thus strongly favouring longer plates for a given deflection angle.

β-NMR

The β-NMR spectrometer requires the ^{8}Li beam to be injected into solenoidal fields up to 9 T, and down to zero. Experimenters also requested implantation energies up to 90 keV and down to as low energy as possible, preferably below 1 keV. The case of spatially-varying coaxial magnetic and electric fields was treated theoretically and incorporated into the beam optics code. The results of studies varying the location and shape of the axial electric field are that to avoid a large beam spot on the sample, the deceleration must occur as close to the sample as possible, and the deceleration electric fields must be as small as possible, but inside the magnetic field. Even so, for reasonable efficiency as regards the fraction of beam implanted on the sample, the product of final beam energy and solenoidal field must be above roughly 1 keV T. As examples, 100 eV implantation energy can be achieved only if the solenoid field is greater than roughly 10 T; solenoidal fields as low as 0.1 T can be achieved as long as the implantation energy is greater than roughly 10 keV.

Commissioning

From the mass separator to the low temperature nuclear orientation (LTNO) experiment there is roughly 40 metres of low energy beam transport (LEBT) consisting of 99 electrostatic quadrupoles and 13 45° electrostatic bends. An emittance scanner at the separator mass slit was used to measure the phase space there, and a tune to match to the rest of the LEBT was calculated. A crucial ingredient of the calculation is the effective length of the standard ISAC (1 inch bore radius) electrostatic quadrupole. This had been measured in 1998 during commissioning of the LEBT section joining the off-line ion source to the RFQ. Using only theoretical settings for the quadrupoles downstream of the section matching the separator to LEBT, beam was transported to the collimator just upstream of LTNO. The fraction of beam reaching this collimator was greater than 90%; consistent with losses expected from interaction with the background gas. Beam profiles measured using scanning wires were substantially in agreement with theoretical values. Fine tuning of the optics consisted mainly of adjusting the steering correctors, especially those adjacent to the 45° electrostatic bends.

In the fall, the polarizer was moved from the test-stand to the ISAC experimental hall. In December, unpolarized ^{8}Li$^+$ beam was successfully guided through the new LEBT section to the Na neutralizer, the He ionizer, and to the β-NMR experimental apparatus. The beam size was well controlled, even though only one of the Einzel lenses was operative. Without ultra-high vacuum in the region of the β-NMR solenoid, it was not possible to power the other Einzel lens. This tuning flexibility is due to the excellent emittance of the charge-exchanged beam.

RF SYSTEMS

RFQ

The ISAC RFQ is an 8 m long, 4-rod split-ring structure operating at 35 MHz in cw mode. The rods are vane-shaped and are supported by 19 rings spaced 40 cm apart. The rings are unique in that the rf surfaces have been structurally decoupled from the mechanical support structure to improve dynamic stability. The full complement of 19 rings has now been installed and aligned (Fig. 123).

In order to meet the stringent, ±0.08 mm, quadrature positioning tolerance of the four-rod electrodes, the three dimensional theodolite intersection alignment method was used. The alignment results are shown in Fig. 124.

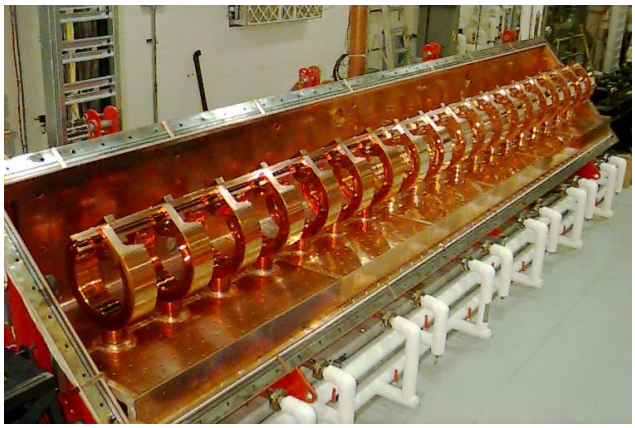

Fig. 123. Full complement of 19 RFQ rings installed and aligned.

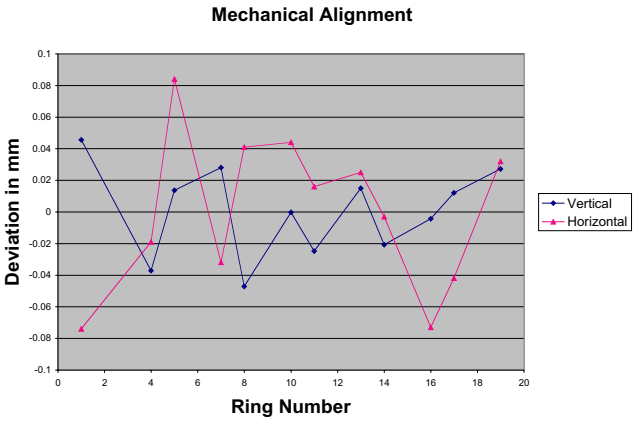

Fig. 124. RFQ mechanical alignment measurements.

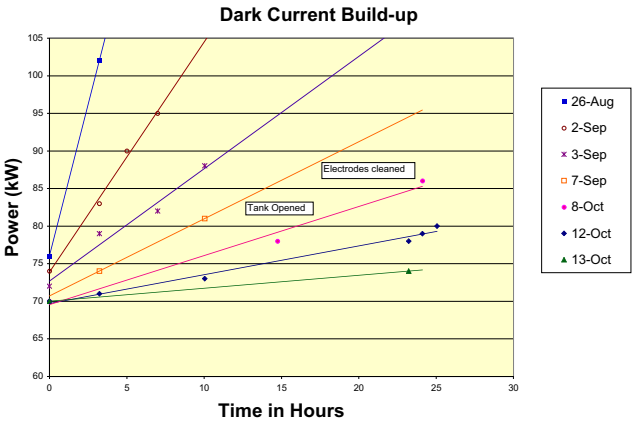

Fig. 125. Increase in power level due to dark currents. The slope of the line determines the growth rate of dark currents.

A relative field variation along the 8 m of the RFQ was measured to be within ±1%, using the standard bead pull method. Signal level measurements gave a frequency of 35.4 MHz, a Q of 8,700 and a resonant shunt impedance of 283 kΩ m. Careful cleaning procedures and high power pulsing reduced the growth rate of dark currents associated with field emission by two orders of magnitude. The gradual reduction of dark currents is indicated in Fig. 125 by the reduction of the slope of the sequential graphs, which are in chronological order. With no dark currents present, the power requirement to reach an inter-electrode voltage of 74 kV is 78 kW. The amplifier is capable of 150 kW for peak power pulsing.

MEBT Rebuncher

The 35 MHz rebuncher is a spiral two gap cavity. The spiral is NC machined from solid copper and water pipes are soldered to the inner and the outer surfaces of the spiral. The spiral, housed in a 36 in. diameter tank, at the open end supports the drift tube and has a stem support at the bottom, as shown in Fig. 126.

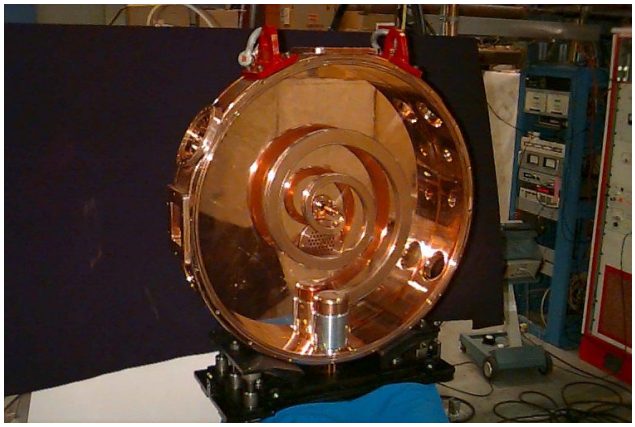

Fig. 126. MEBT spiral rebuncher cavity.

The resonant frequency and Q of the cavity were within 1% and 65% respectively of the value predicted by MAFIA 3D simulation. A 2% change in resonant frequency can be obtained by varying the diameter of the spool piece, which is part of the stem. A fine tuner with a tuning range of 80 kHz is employed to compensate for the frequency change during operation. The shunt impedance and Q were measured to be 490 kΩ and 3,700 respectively. RF power of 1 kW cw was required to obtain the specified nominal tube voltage of 30 kV at the tube. Stable operation at full power was maintained for 36 hours without any interruption.

DTL System

The first DTL tank, with the stems and ridges installed and aligned, is shown in Fig. 127. The ridges are mechanically fastened to the tank wall and therefore the fabrication tolerance on the flatness and surface finish of the bottom of the ridges and the mounting surfaces on the tank wall are very stringent in order to ensure a good electrical contact.

The frequency was measured to be 3.5% higher and the Q to be 20% lower than the values from MAFIA simulations. A bead pull measurement shows the field

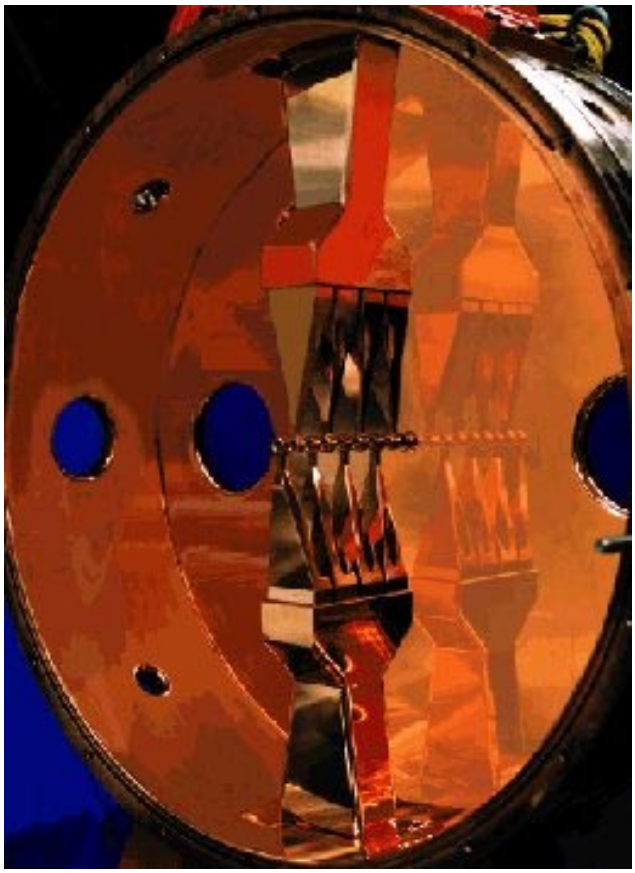

Fig. 127. The first DTL tank with the stems and ridges installed and aligned.

variation across the gaps to be in close agreement with MAFIA simulations, causing only a ±0.1% phase error of the beam at the gap. A coarse tuner was designed to bring the frequency down to the nominal value of 105 MHz. A fine tuner with a tuning range of 180 kHz was also installed. Full power of 3.2 kW and 86.7 kV tube voltage was achieved following 6 hours of low level multipacting conditioning. Stable operation was maintained for 138 hours at full power.

The remaining four tanks have been designed and will be going out for manufacturing in the new year.

RF Amplifiers

The first 4 of 8 power amplifiers for the DTL bunchers and cavities were successfully tested into a resistive load. The remaining 4 are being assembled and readied for power tests.

HEBT Bunchers

Two bunchers, a low beta 11.7 MHz and a high beta 35 MHz, are required for the ISAC high energy beam transport (HEBT). Conceptual designs of these two bunchers were started.

The 11.7 MHz low beta (2.2%) buncher requires a total effective voltage of 100 kV. Using a three gap structure, the tube voltage required is 30 kV. Since the frequency is low, a lumped element coil and drift tube capacitance will form the resonant circuit. The coil will be housed in an air box whereas the drift tube, located in a vacuum tank, will be connected to it via an rf feedthrough. Prototype work has started on the basis of the above conceptual design.

The 35.0 MHz high beta (3.2%) buncher requires a total effective voltage of 255 kV. A two gap structure with tube voltage of 170 kV will be sufficient to provide the required total voltage. Preliminary calculations showed that the MEBT spiral, with certain modifications, can be used for this HEBT buncher. Detailed calculations and design are being done to meet the specifications of the buncher.

ISAC RF Controls

Further refinements were done to the software and hardware of the RFQ rf control. This includes semi-automatic setting for use in pulsed power conditioning, as well as remote monitoring of pertinent rf parameters. Since the actuator of the frequency tuning system was changed from dc motor to stepping motor, the tuning control system was redesigned to accommodate this change. The frequency tuning system will be tested under power at the first available opportunity. Another two control systems were completed in preparation for the re-buncher and the first DTL. These are housed in a VXI mainframe and are similar in design to the RFQ and the prebuncher control system. However, instead of using an embedded processor as the slot-0 controller, a firewire (IEEE 1394) slot-0 controller is used instead and controlled by a stand-alone PC located close by. This offers more flexibility in further system upgrades as well as reducing the cost of each system.

RFQ 19 Ring Test

The final RFQ electrodes span 7.6 m with 19 modules, each consisting of one ring and 40 cm of electrodes. In 1998 an interim beam test was completed with the first 7 ring section (2.8 m) accelerating beams to 55 keV/u. In 1999 the final 12 rings have been added and commissioned with beam. Both rf and beam tests have been successfully completed. The RFQ was operated in cw mode for all beam tests. The operation of the RFQ at peak voltage (74 kV) is stable. A summary of the RFQ rf tests is given earlier in this section on page 147. Beams of both N^+ and N_2^+ have been accelerated to test the RFQ at both low and high power operation.

The test diagnostic set-up is shown in Fig. 128. The first section of MEBT, consisting of five quadrupoles and two steering magnets, is installed with temporary diagnostic boxes placed immediately downstream of the RFQ and downstream of the fifth quadrupole. The upstream box measures the total transmission and beam position emerging from the RFQ and the second box measures the intensity and the beam profile of the accelerated beam. The five quadrupoles act as a velocity filter to remove the non-accelerated beam.

Beam capture as a function of RFQ vane voltage measurements have been completed for each ion and for both unbunched and bunched input beams. The results are given in Fig. 129 (squares) along with predicted efficiencies based on PARMTEQ calculations (dashed lines). The RFQ capture efficiency at the nominal voltage is 80% in the bunched case (three harmonics) and 25% for the unbunched case, in reasonable agreement with predictions.

The longitudinal acceptance was measured. The energy of the injected beam was varied at the source.

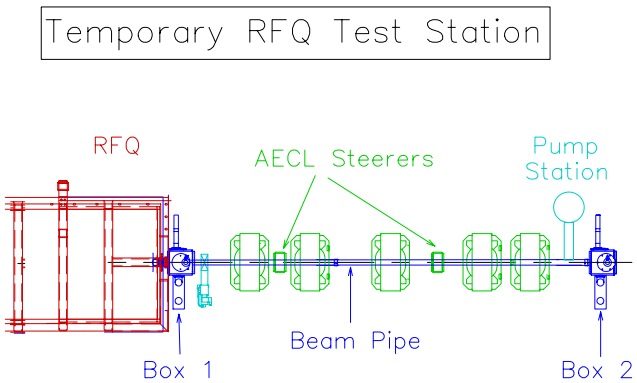

Fig. 128. Experimental test station for initial RFQ 19 ring beam test.

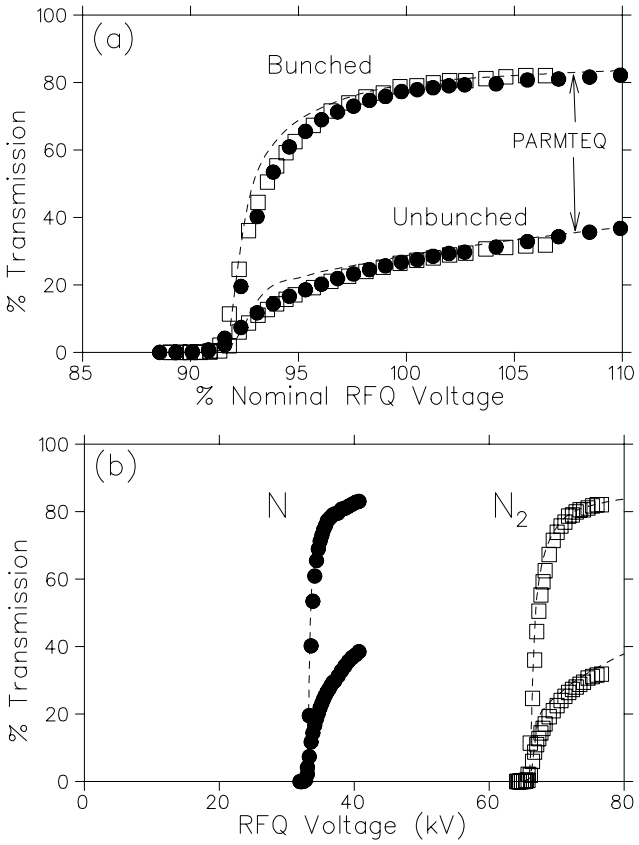

Fig. 129. (a) RFQ beam test results showing capture efficiency for beams of N^+ as a function of relative vane voltage. The beam capture for both bunched and unbunched initial beams is recorded (squares) and compared with PARMTEQ calculations (dashed lines). In (b) the results for both N^+ and N_2^+ are plotted with respect to absolute vane voltage.

For each energy step, the phase of the bunched beam was varied with respect to the RFQ phase and the capture efficiency was recorded for each step. The settings where the acceptance dropped to 50% of the peak value were used to define the longitudinal acceptance contour. The acceptance of the centred beam was estimated to be 180 π % deg at 35 MHz or 0.3 π keV/u ns. Beam transmission contours for both the initial 7 ring configuration and the final 19 ring configuration are presented in Fig. 130. The tail in the acceptance plot seen in the upper right corner of the stable region is typical of linear accelerators.

In general the beam test results compare favourably with the previous 7 ring test and beam simulations. The second RFQ beam test (Test #2) will occur early next year during MEBT commissioning.

RFQ Frequency

It has been determined that the RFQ frequency will be 35.36 MHz as opposed to the design frequency of 35 MHz. The implications of this choice on the beam

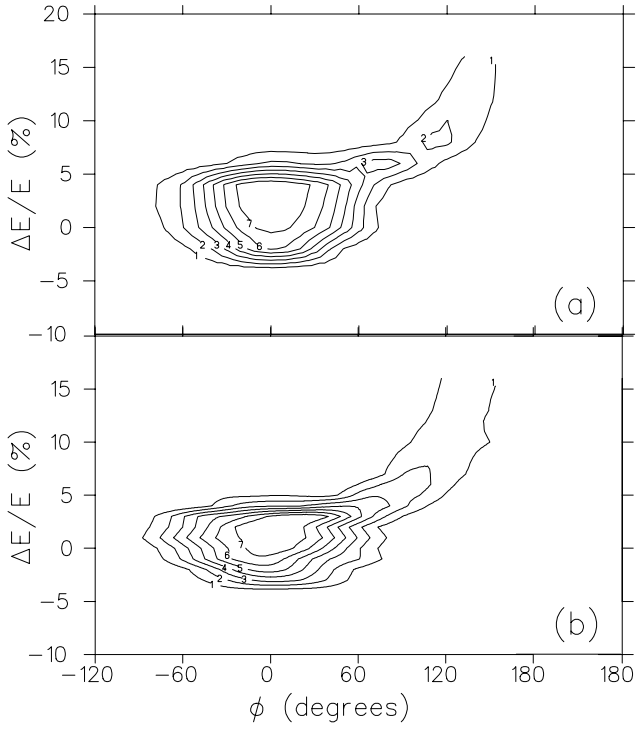

Fig. 130. Measured longitudinal acceptance of the RFQ for the initial 7 ring configuration (a) and for the final 19 ring configuration (b).

dynamics has been considered. In general, as long as the energy change per cell is much less than the particle energy, synchronism can be maintained by adjusting the particle input velocity and the linac voltage. For the case in question, $f_n = 35.36$ and $f_o = 35$, the incident velocity must be 1% higher (incident energy 2% higher) and the accelerating voltage 2% higher than designed. Similarly, the RFQ exit energy and DTL maximum energy are 2% higher than designed or 153 keV/u and 1.53 MeV/u respectively.

MEBT INSTALLATION

Preparations for the installation of the MEBT beam line began in earnest in early 1999. The configuration of this line is shown in Fig. 134.

In early spring, thirteen of the Chalk River quadrupoles were selected for installation in this line. These were moved to the magnet measurement area of the cyclotron building where they were all field-mapped and their effective lengths were measured. By the time these measurements had been completed, the two 45° dipoles for the charge-selection section had been delivered to TRIUMF. These were also field-mapped and their effective lengths were measured.

The basic stand assembly was designed, manufactured and in place by summer. During the summer the first five quadrupoles were installed. The diagnostic station described on page 161 of last year's Annual Report was installed at the location of the MEBT

stripper foil. The vacuum system from the RFQ exit to that point was completed together with associated electronics and control paraphernalia. By fall the line was ready for full power RFQ tests. This test and its results are summarized in another section.

Work continued toward completion of the remainder of the beam line. Design of the dipole vacuum vessels and stands was completed and these were sent out for manufacture. The remaining quadrupoles of the beam line were mounted and aligned.

Because of the compactness of the charge selection system it was necessary to design 3 compact steering magnets. Two of these are vertical steering; the third has both horizontal and vertical steering capability. These were engineered and sent out for manufacture. The completed units were received late in the year.

In addition to these steerers, steering windings were requested on the middle two quadrupoles of the quadruplet that lies downstream of the rebuncher. Consequently, this unit was removed in preparation for the installation of these windings.

By the end of the year great strides had been taken toward a second test in the early spring of 2000. In this test, beam will be brought to the location of the rebuncher so that the charge distribution from the stripper foil and action of the charge selection system may be studied.

BUNCH ROTATOR STUDY

A bunch rotator is specified for the matching/chopping section of MEBT just downstream of the RFQ. The device provides a time focus on the stripping foil to reduce the longitudinal emittance growth due to energy straggling during stripping. It was decided to utilize the DTL prototype buncher for this application. The device is a three-gap split-ring buncher operating at 105 MHz. The new application requires alteration of the buncher in two ways. Firstly, the design β of the drift tube gaps must be altered from 2.3% to 1.8% to match the MEBT beam velocity. Secondly, the aperture of the drift tubes must be increased from 14 mm to 25 mm since the beam optics in the section demand that the beam is relatively large in the bunch rotator. The device is 98 mm in the beam direction from inside face to inside face. The design velocity demands a gap to gap distance of 25.7 mm giving the drift tube geometry shown in Fig. 131.

It is clear that the ratio of gap to aperture is very low. This yields a low transit time constant of 0.56 for on-axis particles and enhances radial-longitudinal coupling effects since the transit time improves off-axis to a maximum of 0.9 at the full beam aperture. These possible complications led to a beam dynamics simulation of the bunch rotator. The geometry shown in Fig. 131 was simulated using RELAX3D. An

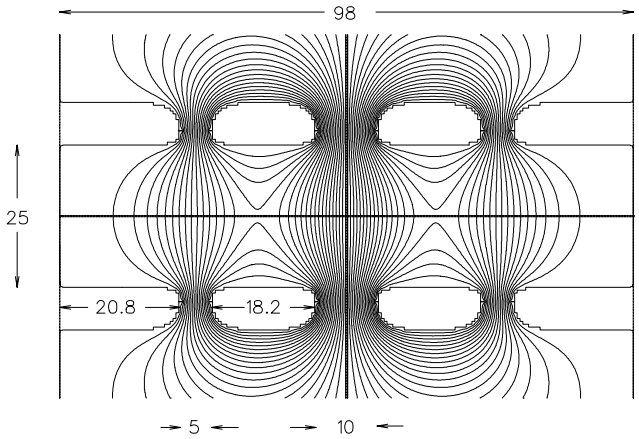

Fig. 131. Drift tube geometry for the MEBT bunch rotator.

ensemble of 5,000 particles with a normalized transverse emittance of $\beta\epsilon_{x,y} = 0.1\ \pi$ mm mrad was accelerated through the RFQ and MEBT matching section. The position of the particles in longitudinal phase space was calculated at the position of the stripping foil for three different cases: rotator off, rotator on with a zero emittance beam, and rotator on with a normal emittance beam. The zero emittance case removes any radial coupling effects. The results of the longitudinal study are shown in Fig. 132. It is clear from the results that the large aperture of the device, coupled with the large beam size, does affect the longitudinal phase space, leading to an RMS emittance growth of 12%. However, the large reduction in the time spread over the rotator off case and the inherent reduction in energy straggling will more than compensate for this small growth. Beam simulations concerning transverse motion are summarized in Fig. 133.

In summary, the horizontal plane experiences a 1% growth in RMS transverse emittance while the vertical plane increases by 4%. These levels of growth are acceptable. The final specifications for the bunch rotator are presented in Table XVII.

Table XVII. Bunch rotator specifications assuming $A/q = 30$.

Parameter	Value
RF frequency (MHz)	105
β_o (%)	1.8%
λ (m)	2.85
$N_{\rm gap}$	3
$\beta\lambda/2$ (mm)	25.7
$V_{\rm eff}$ (kV)	60
$V_{\rm tube}$ (kV)	27
$\sim L$ (mm)	98
$L_{\rm tube}$ (mm)	18.2
$L_{\rm gap}$ (mm)	5, 10
Full beam aperture (mm)	25
T_o (on axis)	0.56

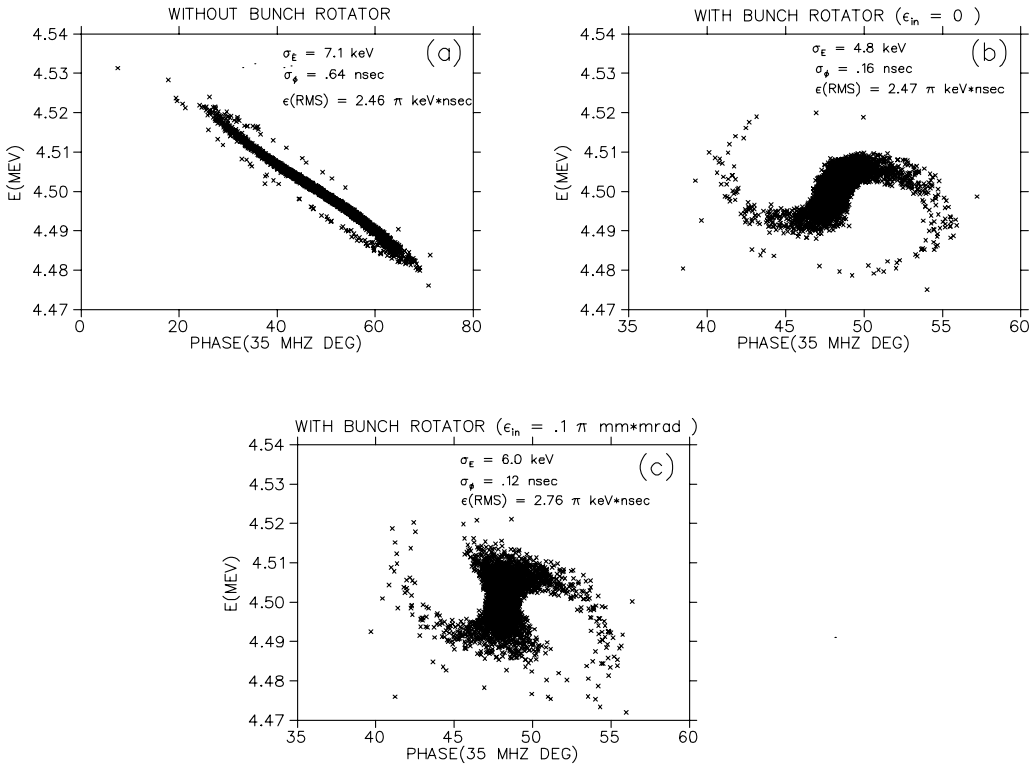

Fig. 132. Particle positions in longitudinal phase space at the MEBT foil location for three simulated cases: (a) bunch rotator off, (b) rotator on with $\beta\epsilon_{x,y} = 0$, (c) rotator on with $\beta\epsilon_{x,y} = 0.1\ \pi\,\mathrm{mm\,mrad}$.

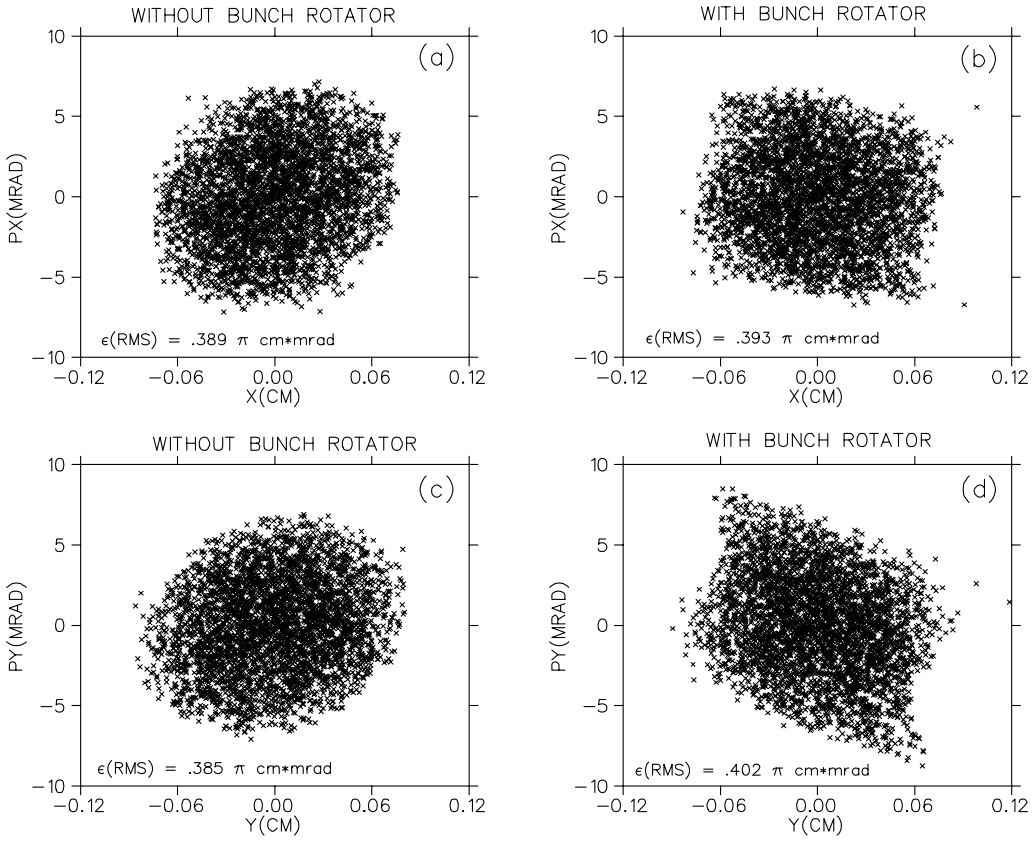

Fig. 133. Particle positions in transverse phase space at the MEBT foil location for the bunch rotator off and on. Plots (a) and (b) show the 'x' phase space and plots (c) and (d) show the 'y' phase space.

MEBT CHOPPER

Introduction

Since the beam is bunched at 11.7 MHz but not chopped before the 35 MHz RFQ, there is a small amount (∼3.5%) of beam accelerated in the 35 MHz buckets on either side of the main bunch. These bunches contaminate the time structure and must be removed to achieve the design bunch spacing of 86 ns. There is also a request that for certain experiments the time spacing be increased to double this, i.e., 172 ns, by eliminating every second main bunch as well as the satellite bunches. A chopper has been conceptualized for the matching section of MEBT (Fig. 134).

The chopper plates are positioned between the third and fourth quadrupoles. The optics are chosen to give a broad low divergence waist at the chopper plates in the selection plane and a 90° transverse phase advance to the chopper slits located near the stripping foil. In this way a small deflection at the chopper plates produces a displacement of the deflected beam at the chopper slits.

Chopper Concepts

Various chopper concepts that allow both modes of operation were investigated. Concept I comprises a single frequency, single plate option where the chopper operates in classic sine-wave configuration to achieve Mode A (86 ns) timing and with one plate biased in an off-set cosine-wave configuration to achieve Mode B (172 ns) timing. Concept II is a dual frequency single plate option where both Mode A and Mode B used an off-set cosine-wave approach. Concept III is a dual frequency dual plate approach with each plate pair operating in an off-set cosine-wave configuration.

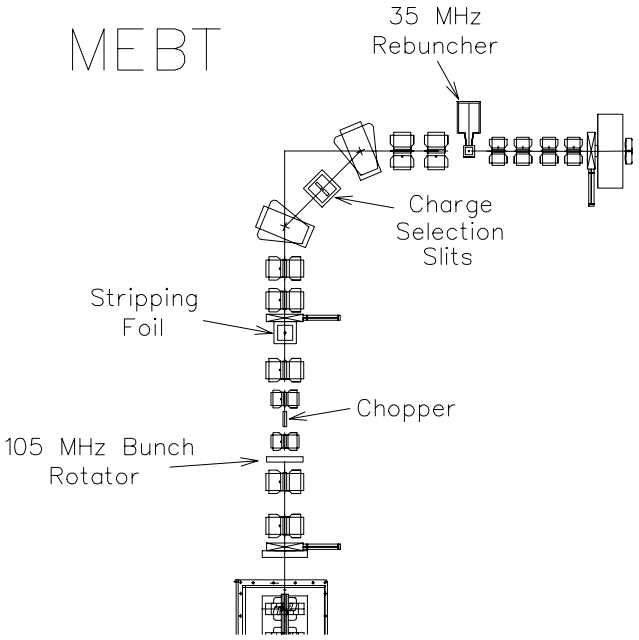

Fig. 134. ISAC medium energy beam transport (MEBT).

It was found that for this application the sine-wave configuration, even for a well-bunched beam, leads to transverse and longitudinal emittance growth. It is the latter that experiences the largest relative emittance growth since the longitudinal phase space is not upright at the chopper plates. This is of concern since considerable efforts have already been expended in the RFQ and bunch rotator design to keep the longitudinal emittance small. In addition, the 86 ns Mode A case that produces the most emittance growth will be the most common mode of operation since it provides the most beam intensity. The reduced phase width that comes with the installation of the bunch rotator helps to reduce the negative effects of the sine-wave chopper, however, a growth of 75% is still expected. This is too high. One way to reduce the effects of the sine-wave chopper on energy spread growth is to feed the plates symmetrically, but this is a more complicated hardware solution. Voltage regulation between the plates poses a challenge.

Concept II greatly reduces problems of emittance growth but demands a second amplifier at a different frequency to achieve the two modes of operation. The voltage required on the plates in the Mode B timing case is quite high at 20 kV. This voltage is required to achieve at least 6 kV for the two satellite bunches on either side of the main bunch.

In Concept III the voltage is reduced dramatically by adding a separate pair of plates downstream of the first to operate in tandem. In this way the first plates produce Mode A timing when excited at 11.7 MHz. To switch to Mode B timing the first plates are left on as before and the second set are powered at 5.8 MHz with a voltage only sufficient to deflect the unwanted main bunch. Two amplifiers at different frequencies are still required, but the voltages are now each below 10 kV. The longitudinal space required is twice that for the single plate solution, but this could be reduced at the expense of somewhat higher voltages. The tolerances on operation in this mode are not stringent and should be able to be met through standard TRIUMF rf control.

Concept III Studies

The Concept III option comprising two sets of plates driven at two different frequencies was chosen. Each set of plates has one plate driven at radio frequency and the other at a dc bias equivalent to the peak rf field so that the deflecting waveform oscillates from 0 to 2 V_{dc} (Fig. 135).

Mode A (86 ns) operation is achieved by removing the low intensity satellites with 11.7 MHz rf. Mode B

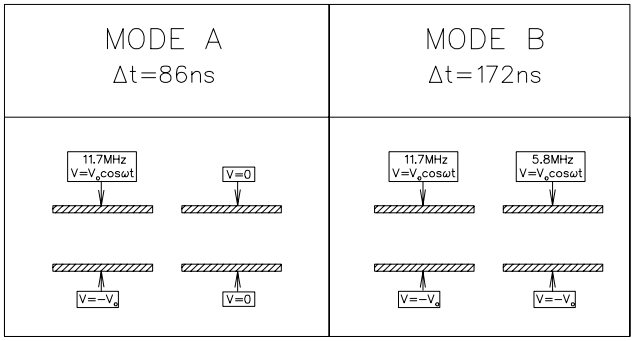

Fig. 135. A schematic of the Concept III two-mode tandem chopper configuration.

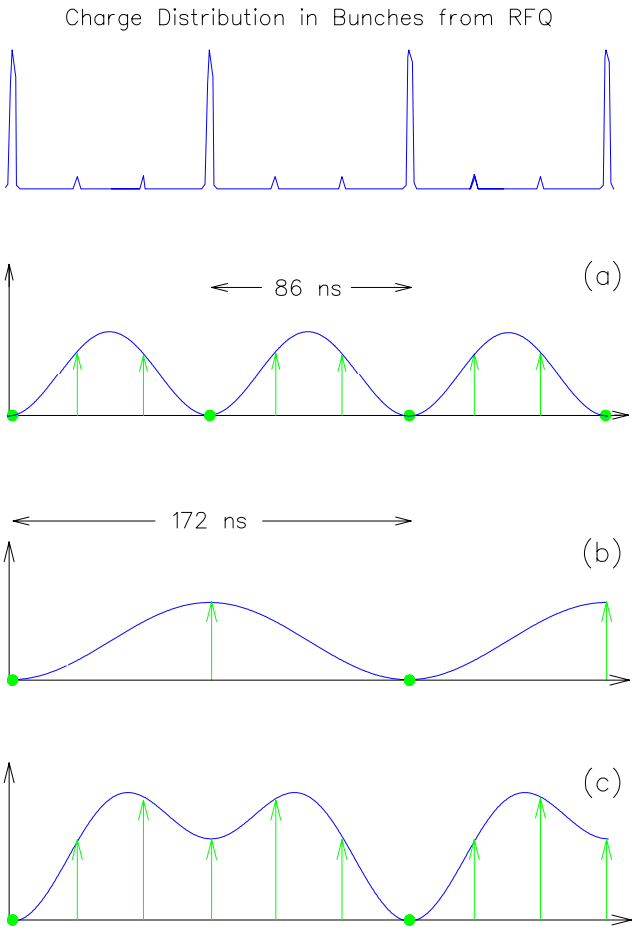

Fig. 136. A schematic of the two-mode tandem chopper waveforms. The charge distribution in the RFQ bunches is shown in the top plot. For Mode A the first set of plates is excited with an 11.7 MHz deflecting voltage as shown in (a). For Mode B the second set of plates is also excited at 5.8 MHz as shown in (b). The total resultant deflection is shown in (c).

(172 ns) timing is achieved by operating the first set of plates at 11.7 MHz to remove the satellites and the second set at 5.8 MHz to remove every second bunch. A schematic of the waveforms for the chopper is given in Fig. 136.

Care must be taken that both plates kick in the same way so that the second plates don't reduce the deflection from the first set. Note that in the case where the second set of plates are excited, the voltage on the first set can be reduced since the two waveforms add.

Electrostatic models of the plate geometry are calculated using RELAX3D. To generate the initial distribution for the Monte Carlo study, a particle ensemble consisting initially of 5,000 particles at the design emittance of 50 π mm mrad is pre-bunched with three harmonics in a LEBT simulator then accelerated through the RFQ. The resultant ensemble then passes through the MEBT optics including the chopper plates and is analyzed at the chopper slit location. A second set of calculations was performed with a larger emittance of 100 π mm mrad to check if the chopper parameters were sufficient to transfer this larger beam.

A summary of the transverse and longitudinal phase space simulations at the position of the chopper slit are shown in Fig. 137 for a set of plates each 7.5 cm long. The increase in the transverse and longitudinal emittance due to the chopper is less than 1%. Note that the small lens effect in the plate geometry has produced a tilt in the transverse phase space. This could easily be corrected by a slight retune of the quadrupole settings.

Chopper Specifications

The final specifications for the chopper are presented in Table XVIII. A schematic of the recommended plate geometry is shown in Fig. 138.

The physical length of the plates is chosen to fit into the available space and produces an effective length of 66 mm. The length of the entire assembly is about 180 mm.

Table XVIII. Summary of chopper specifications.

Parameter	Mode A	Mode B
Δt (ns)	86	172
Mode	Cosine-wave	Cosine-wave
Frequency (MHz)	11.7 MHz	5.8 MHz
Plate 1A	7.4 kV rf	5.5 kV rf
Plate 1B	−6.8 kV dc	−5.1 kV dc
Plate 2A	0 kV	5.5 kV rf
Plate 2B	0 kV	−5.1 kV dc

CHARGE DISTRIBUTION AND BEAM LOSS AFTER MEBT FOIL

The stripping foil in the MEBT increases the charge of the exiting ions to reduce the total voltage required in the DTL. The expected distribution of charge states over the ISAC mass range is important to estimate stripping efficiency and to predict the location of beam loss in the charge selection region of MEBT.

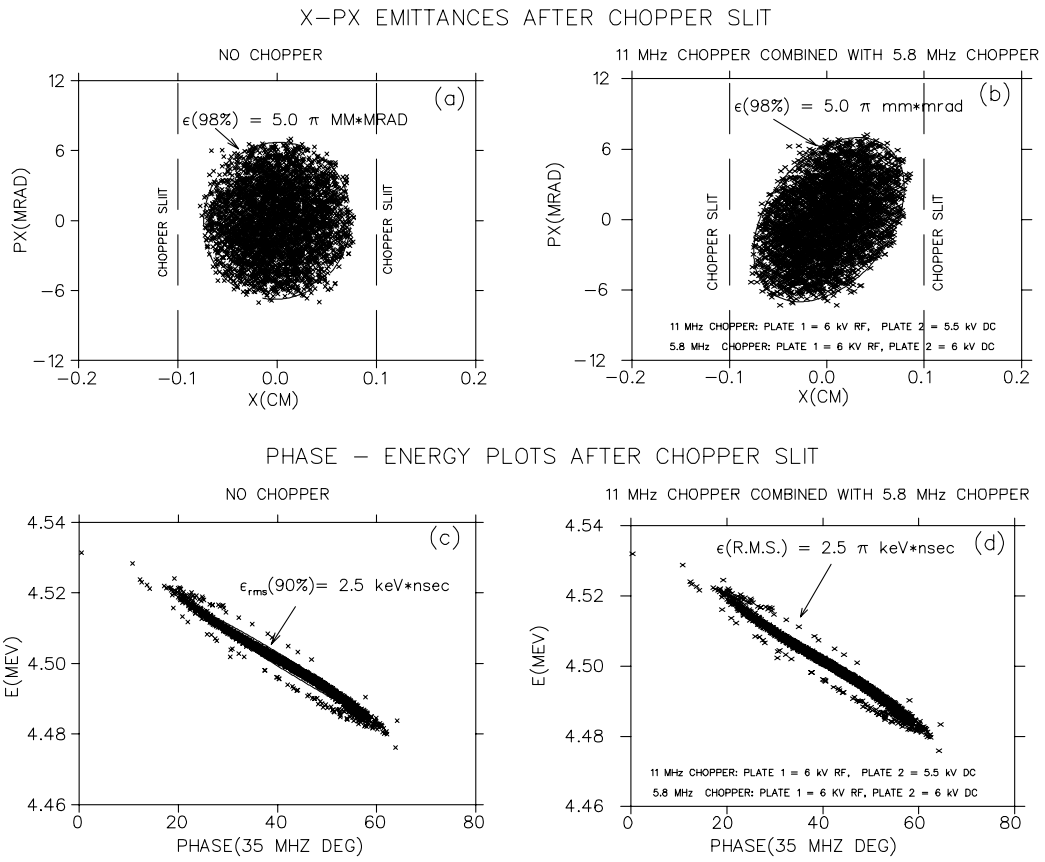

Fig. 137. Summary of transverse and longitudinal phase space simulations at the chopper slit location for (a,c) no chopper, (b,d) 5.8 MHz/11.7 MHz tandem cosine-wave chopper.

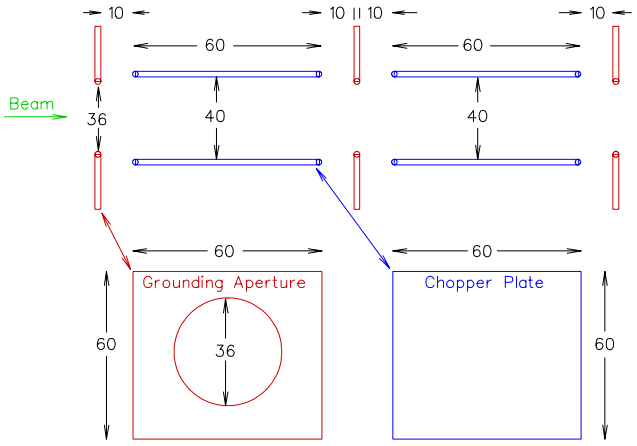

Fig. 138. Schematic drawing of chopper plate assembly. Dimensions are in mm.

Reference data concerning equilibrium charge fractions emerging from a stripping foil are applied to the ISAC case. The data are used to get charge distributions at 150 keV/u for various masses. The results are plotted in Fig. 139 as a function of charge to mass ratio. We have assumed that $A = 2Z$. The charges associated with each point are shown on the plot.

The charge state distributions are used to predict where ions not selected for transmission are lost in the MEBT. The charge selection dipole is set to transmit the optimum charge state. The radius of curvature, ρ, is proportional to A/q and so the other charge states will be lost in the dipole vacuum chamber, beam pipe, or charge selection slits.

To get an idea of a possible beam loss history, the data in Fig. 139 is summed keeping the most significant losses, and a summary distribution is calculated and plotted in Fig. 140. The data are given as the fraction of ions with ρ/ρ_o, where ρ_o is the design radius of curvature for the dipole.

To estimate regions of beam loss, the important ion rigidities shown in Fig. 140 are geometrically constructed on a layout of the MEBT dipole and vacuum chamber. This plot is shown in Fig. 141. The plot shows that all ions except for those with the most probable charge state will be lost in the dipole vacuum chamber or beam pipe.

The beam loss is quite localized and so shielding requirements are relatively straightforward. The magnet itself will provide shielding, plus small lead blocks may be inserted along the beam pipe between the field clamp and the magnet pole. Shielding of the charge selection slits box may not be required.

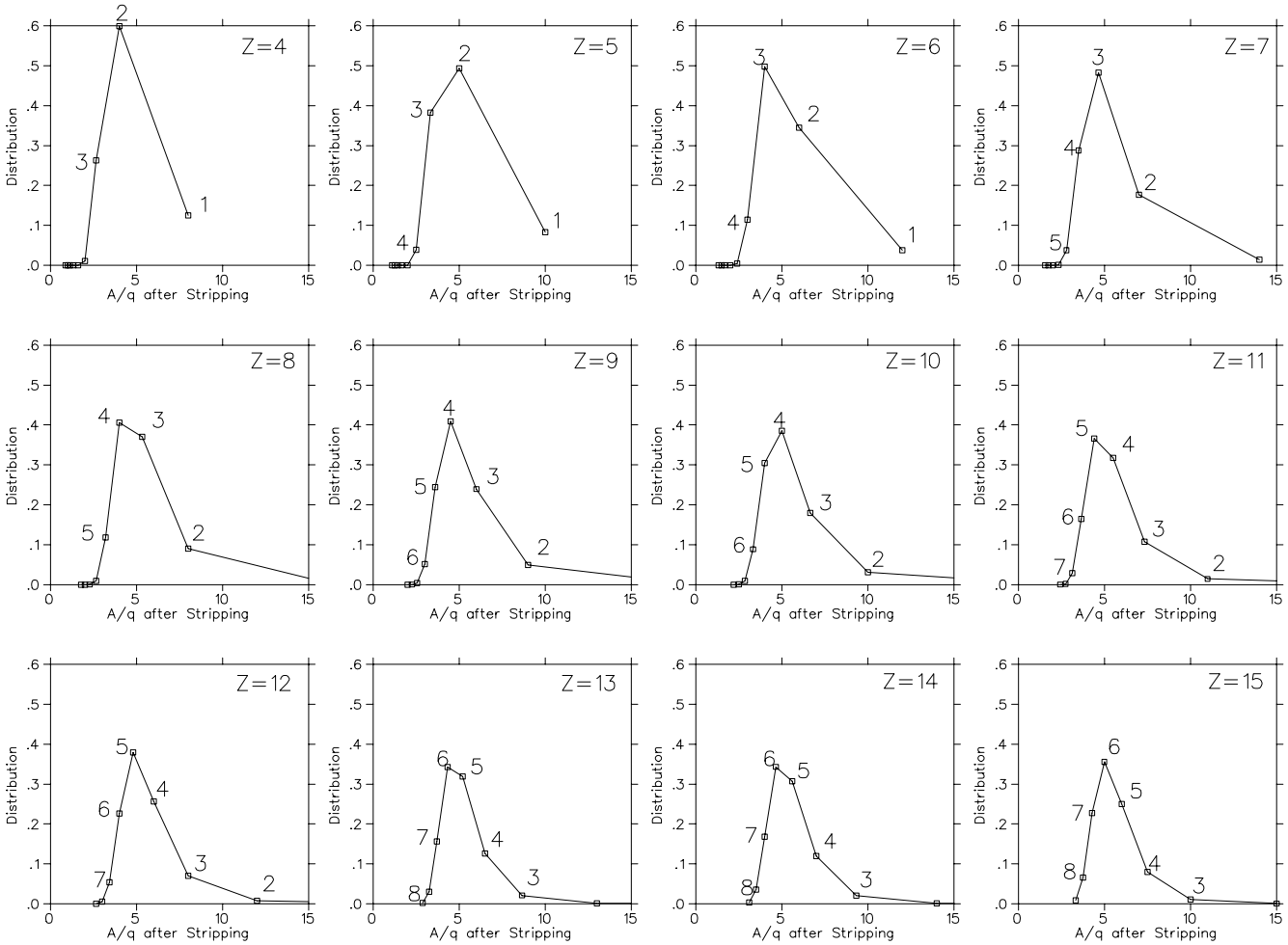

Fig. 139. Distribution of mass to charge ratio emerging from carbon foil for ions with Z = 4–15 at 150 keV/u. Labels indicate the charge, q, of a particular ion.

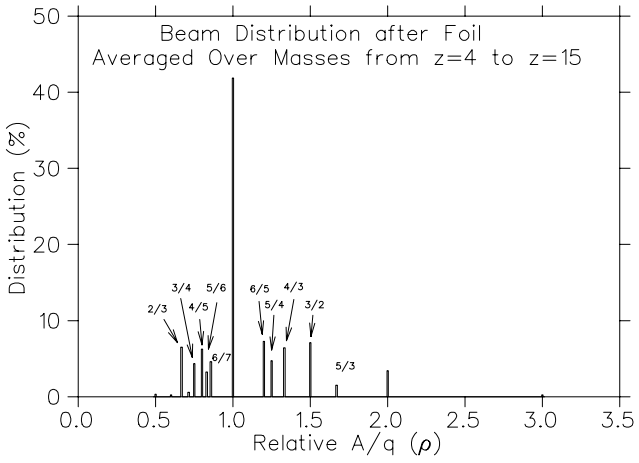

Fig. 140. Percentage distribution of ion rigidity averaged over Z = 4–15 at 150 keV/u compared to design rigidity.

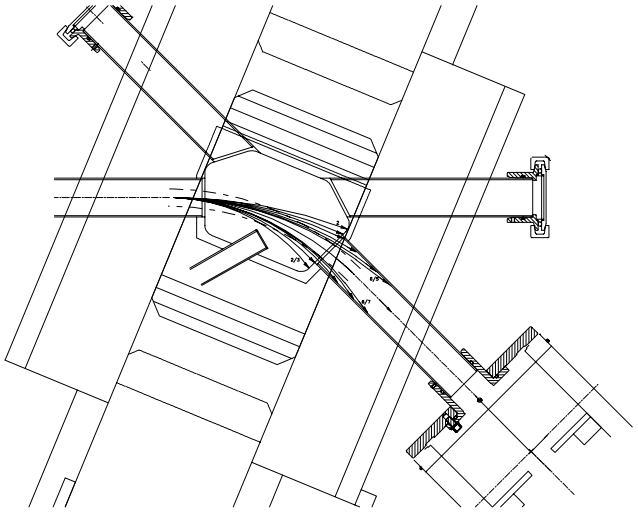

Fig. 141. Beam trajectories in MEBT dipole showing locations of beam loss.

HEBT DESIGN

Introduction

The ISAC high energy beam transport (HEBT) takes beam from the ISAC DTL and delivers beam to various target stations. The specifications for the HEBT were defined including those for the transverse optics, beam bunchers, steering requirements and diagnostics. The aim in the HEBT design is to transport the beam to the experimental stations with little or no beam loss and emittance growth, provide a flexibility in the transverse and longitudinal 'spot' size at the target, and allow for 'cleaning' of the beam if required.

A schematic of the HEBT layout is shown in Fig. 142. The E-W line from the DTL acts as a central trunk with achromatic 45° bending sections spaced evenly along this line delivering the beam to up to four experimental stations. In the initial HEBT installation the first two bend sections will be installed to deliver beam to the DRAGON and TUDA facilities.

The HEBT is composed of four basic sections:

1. DTL→HEBT matching/chopping section
2. Beam analysis section
3. Periodic/achromatic bend section
4. Matching section to experiment

The first section provides matching from the DTL to the HEBT and includes a chopper insertion if required. A chopper slit would be placed at the two-dimensional focus at the end of this section. The beam analysis section is an optics section that both matches the beam to an energy analysis station and also provides beam transport to the next section. The next part of the HEBT consists of periodic sections with 45° achromatic bends periodically placed down the E-W beam line. Each achromatic bend section ends in a matching section to produce the correct transverse beam shape on target.

Longitudinal Optics

Beams emerging from the DTL will range in energy from 0.15–1.5 MeV/u. The energy spread inherent in the beams will cause debunching as the particles are transported down the HEBT. The position and frequency of the HEBT buncher(s) should be such that the time spread of the beam bunch is no more than $\omega\Delta t \leq \pm 45°$ of the buncher rf cycle, or serious longitudinal emittance growth will occur. It is found that two bunchers, a low-β 11.7 MHz buncher for beams from 0.15–0.4 MeV/u, and a high-β 35 MHz buncher for beams from 0.4–1.5 MeV/u, placed ∼12 m downstream of the DTL, can provide efficient initial bunching of all beams from the DTL without longitudinal emittance growth.

There are ∼12 m from the DTL to the bunchers and roughly 11 m, 17 m and 23 m to the first three experimental stations. The bunchers can operate in two different modes depending on the requirements of the experimenter. In both cases the buncher operates on

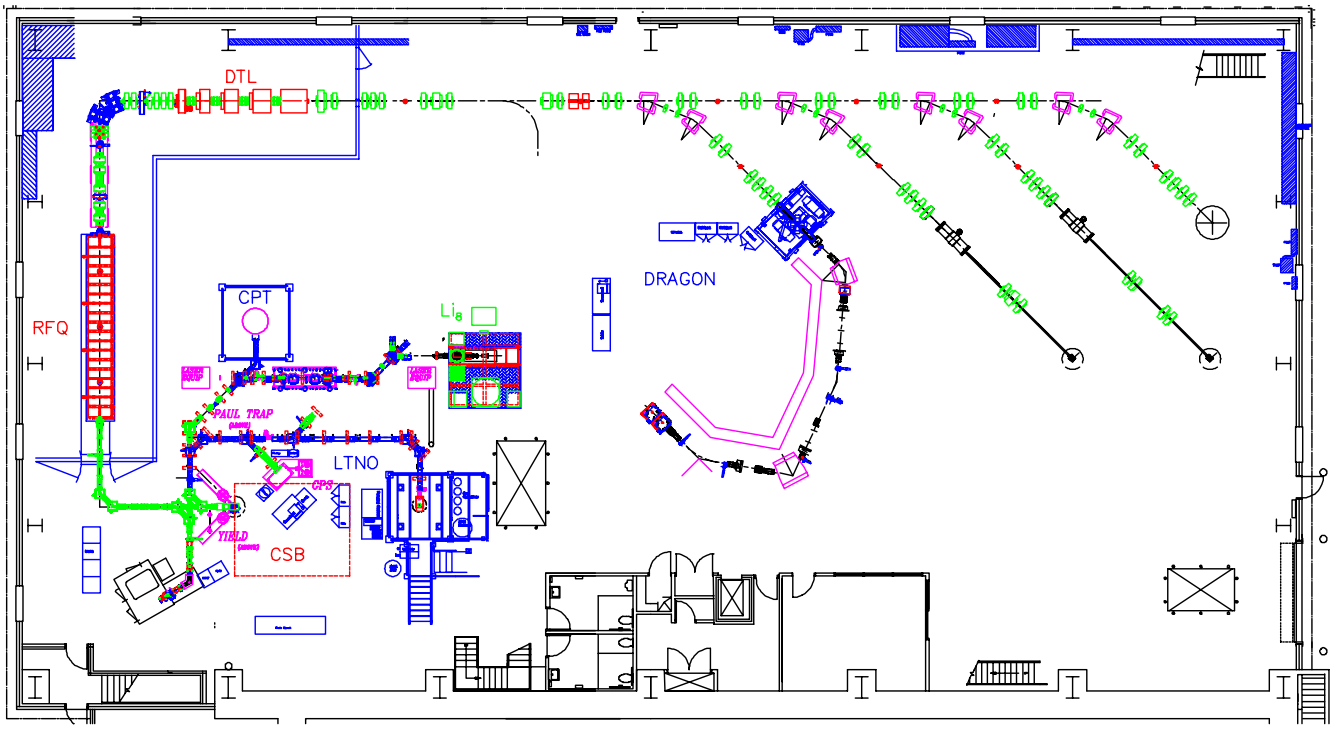

Fig. 142. ISAC experimental hall showing high energy beam transport (HEBT).

the beam that has debunched after leaving the DTL. In the energy focus mode A, the buncher voltage is set to remove the energy spread in the beam emerging from the DTL. The beam on target will have a relatively large phase spread but small energy spread. In the time focus mode B, the buncher voltage is set to re-converge the diverging beam. The beam on target will have a relatively short time pulse but will have an energy spread with a magnitude similar to the beams emerging from the DTL. Since mode A produces an almost mono-energetic beam, further phase spread after bunching will be relatively small so that the longitudinal characteristics will be similar for all experimental stations. In mode B, however, the distance from buncher to target differs depending on the experimental station so that longitudinal beam parameters will vary; closer stations will receive beams of higher energy spread and smaller time focus, while for farther stations the energy spread will be lower at the expense of an increase in the phase width.

The voltage required on the buncher can be estimated from the distances, the beam energies and the frequency of the buncher. A plot of the drift tube voltages assuming two-gap bunchers is shown in Fig. 143 for both mode A and mode B operation. The points mark actual beam simulations. The values used in the graph assume a transit time constant, $T_o = 0.9$. The important parameter is the effective voltage, $V_{\rm eff}$, given by $V_{\rm eff} = 2\ V_t T_o$. From the graph the maximum required values of $V_{\rm eff}$ are 100 kV and 255 kV for the low- and high-β bunchers respectively.

The required tube voltages are dependent on the choice of buncher geometry and the respective transit time constant. We have chosen $\beta_o = 0.022$ as the design velocity of the low-β buncher and $\beta_o = 0.032$ as the design velocity of the high-β buncher. A plot of the

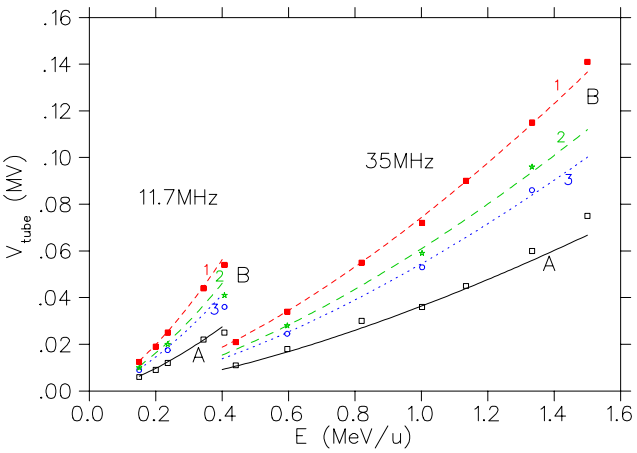

Fig. 143. Required drift tube voltages for both the 11.7 MHz and 35 MHz bunchers for both mode A and mode B operation and for the first three experimental stations 1, 2, and 3.

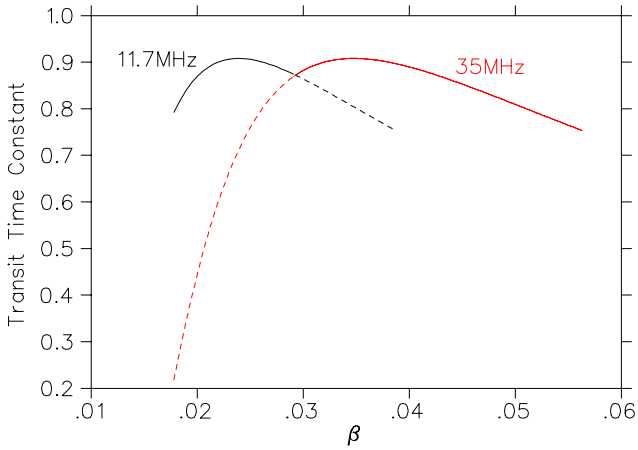

Fig. 144. Transit time constant as a function of ion velocity for both low- and high-β bunchers. The dotted lines show transit times outside of normal range of operation.

respective transit times as a function of ion velocity is shown in Fig. 144. For the highest beam energy and A/q values the low-β cavity would operate over the velocity range indicated by the 11.7 MHz solid line. For ions of less rigidity the cavity could be operated to a higher velocity. In this case the bunching is still reasonably efficient up to 1 MeV/u ($\beta = 0.04$) as shown by the 11.7 MHz dashed line. The choice of the high-β cavity geometry is chosen to give a reasonable efficiency at the highest velocity ($T_o \geq 0.76$) (solid 35 MHz line in Fig. 144), but also allow a flattop mode at lower velocities where the high-β cavity can be used to extend the phase acceptance of the low-β cavity (dashed 35 MHz line).

The final specifications for the bunchers are presented in Table XIX.

Table XIX. Buncher specifications for HEBT assuming $A/q = 6$.

Parameter	Low-β	High-β
RF frequency (MHz)	11.7	35
β_o (%)	2.2	3.2
λ (m)	25.7	8.57
$N_{\rm gap}$	3	2
$\beta\lambda/2$ (cm)	28.3	13.7
$V_{\rm eff}$ (kV)	100	255
Full beam aperture (cm)	2	2

Beam simulations of the specified bunching arrangement were completed for various energies and for experimental stations 1, 2 and 3. A longitudinal emittance of 1.5 π keV/u ns was used in the simulations. Final longitudinal beam characteristics are shown in Fig. 145 and Fig. 146 for mode A and mode B operation respectively. Buncher settings for mode A are the same regardless of the experimental station so only one curve is shown. In mode B the optimized buncher

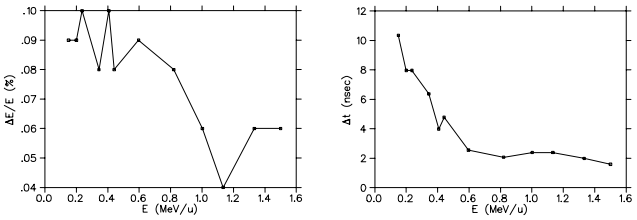

Fig. 145. Final longitudinal beam characteristics for mode A tuning assuming $\epsilon_z = 1.5\ \pi$ keV/u ns.

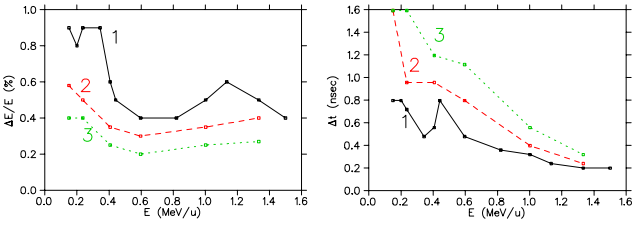

Fig. 146. Final longitudinal beam characteristics for mode B tuning to the first three experimental stations 1, 2, and 3 assuming $\epsilon_z = 1.5\ \pi$ keV/u ns.

setting depends on the drift length to the target so beam characteristics are dependent on the target considered.

Fine Tuning

In the case that an experiment requires different longitudinal beam parameters on target, a buncher could be placed closer to the target. The two bunchers operating in tandem would allow a wide range of possible longitudinal beam characteristics.

In the ISAC HEBT a logical position for the second buncher is the double waist that separates section 3 from section 4. The distance from waist to target varies depending on the required experimental hardware and transverse dynamics requirements, but in general the distance d_3 ≃3–3.5 m. One possibility is to have a 'portable' extra buncher available to be installed when required by the experiment.

Transverse Optics

DTL→HEBT periodic section

A schematic of the first two sections of HEBT is shown in Fig. 147. The positions of the four x–y steerers are indicated in the figure. The total length of these

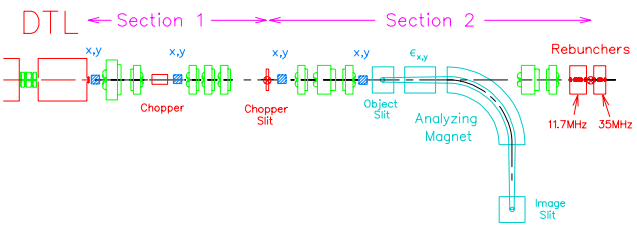

Fig. 147. Schematic of section 1 and section 2 of HEBT.

sections is 11.79 m. A double focus is created at the end of section 2. The low- and high-β bunchers are positioned on either side of the focal point. The length of the two sections, 3.68 m and 8.11 m, is chosen to give comparable maximum beam sizes in each section.

The matching/chopping section takes the diverging beam from the DTL and matches the beam to the standard HEBT double waist with $\beta_{x,y} = 0.02$ cm/mrad. Normally four quadrupoles would be sufficient. In this case five quadrupoles are used with the 'second' quadrupole replaced by two quadrupoles with a drift in between where a low-divergence waist occurs in the horizontal plane. A pair of chopper plates can be positioned in this drift with the chopper slit at the double waist, a 90° phase advance downstream.

The beam analysis section consists of a quadrupole triplet, a diagnostics section, and a quadrupole doublet. The section operates in two modes. The analysis section consists of a 90° analyzing magnet with an object and image slit for energy and energy spread measurements, and a slit and harp transverse emittance rig. In the first mode the first two quadrupoles of the triplet and the doublet quads are used to provide periodic transport from double waist to double waist with a magnification of −1. In the second mode the analyzing magnet is turned on to coincide with a given energy and the triplet is used to focus the beam horizontally onto the object slit while providing a slightly converging beam vertically. The magnet produces a dispersion of 3 cm/%($\frac{\Delta p}{p}$). The beam half envelopes for section 1 and section 2 of HEBT for the two modes of operation are shown in Fig. 148 and Fig. 149.

Sections 3 and 4 of HEBT

Sections 3 and 4 consist of a series of achromatic bend sections linked by a common spine. The bends send the beam to the various experimental stations (DRAGON, TUDA, COULEX, etc.) with each station

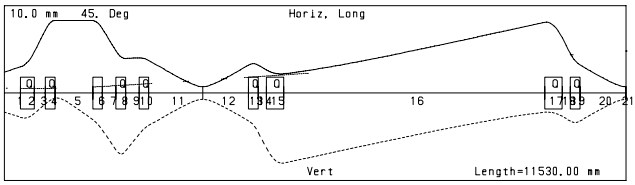

Fig. 148. Beam half envelopes for section 1 and section 2 of HEBT; in periodic mode.

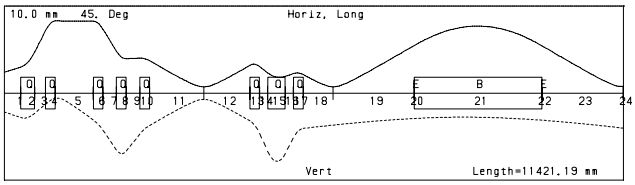

Fig. 149. Beam half envelopes for section 1 and section 2 of HEBT; energy analysis mode.

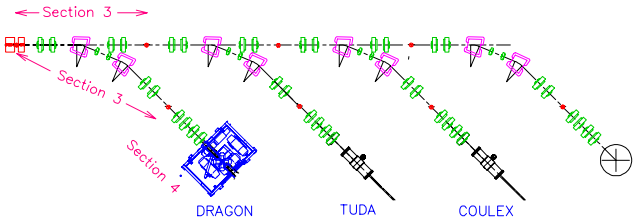

Fig. 150. Schematic of sections 3 and 4 of HEBT.

equipped with a four quadrupole matching section upstream of the target to satisfy particular experimental transverse beam requirements. A schematic of this section of HEBT is shown in Fig. 150.

The periodic/achromatic section consists of identical building blocks. Each section can work in two modes. In the first mode the section is a 6 m long doublet-doublet transport section from double waist to double waist with a magnification of -1. In the second mode the initial doublet forms part of a QQDQQDQQ 45° achromatic bend section that steers the beam towards an experimental area. Beam half envelopes for the two modes of operation are shown in Fig. 151 and Fig. 152.

A horizontal dispersed focus is created in the symmetry plane with a dispersion of 0.44 cm/%($\frac{\Delta p}{p}$). The achromatic bend section can also be operated in a dispersed mode.

Section 4 provides the matching from the double waist downstream of the achromatic section to the target. The optics will be dependent on the experimental apparatus upstream of the target and the beam specifications from the experimenter. In general a four quadrupole system will be used. In the case of the DRAGON facility, the target is a windowless gas target with a large differential pumping system that restricts the beam apertures and does not allow placement of quadrupoles within 130 cm of the target. These

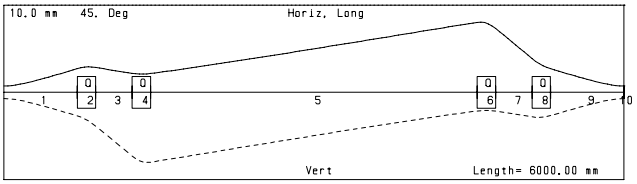

Fig. 151. Beam half envelopes for section 3 of HEBT; periodic mode.

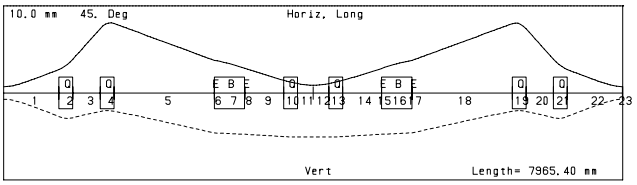

Fig. 152. Beam half envelopes for section 3 of HEBT; achromatic bend mode.

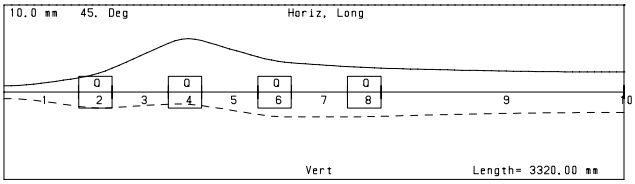

Fig. 153. Beam half envelopes for section 4 of HEBT; the matching section to DRAGON.

restrictions call for a moderate divergence in the beam. The half beam envelopes for this matching section are shown in Fig. 153.

Diagnostics

Initial commissioning and pre-tuning of the HEBT will be done with 'high-intensity' diagnostics capable of operating in the range from 1 nA to 10 μA. Devices required will be Faraday cups (FC) and profile monitors (x, y) for tuning the transverse optics. In general a diagnostic box will be located at each double waist in the beam transport. In addition a set of horizontal selection slits will be located at the dispersed focus between HEBT dipoles. A transverse emittance rig will be installed as part of the diagnostics section before the analyzing magnet.

Timing monitors (Δt) consisting of either fast Faraday cups or other devices will be used to tune the longitudinal optics. One such device is required at the buncher station and also at each double waist upstream of a target station. The energy and energy spread in the beam can be determined with the analyzing magnet. The dispersion of the magnet is 3 cm/%($\frac{\Delta p}{p}$) so that an energy change of 0.1% gives a 1.5 mm change in the beam position at the image position. To achieve this resolution an object slit of 1 mm or less is required. An image slit and Faraday cup or a harp profile monitor can be used to record the horizontal profile at the image position. The energy measurement with the analyzing magnet can be cross-checked with a resonance reaction at various reference energies.

After establishing the energy with the analyzing magnet, the relative energy can be monitored with a time-of-flight system consisting of two phase pick-ups downstream of the buncher. In this way they can serve both to monitor the relative velocity of the beam and to select the phase of the bunchers.

Vacuum Requirements

The cross section for interaction with residual gas atoms is highest at the lowest velocities in the HEBT and these velocities correspond directly to the MEBT energy. The greatest loss rate is for the highest charge state and this corresponds to $q = 6$ ions. The expected loss rate is 0.02%/m at a pressure of 1×10^{-7} torr. The total length of the HEBT depends on the experimental area, but varies from 25–40 m. Taking the worst

case gives an expected loss of 0.8% for 1×10^{-7} torr. If we place a somewhat arbitrary limit of a few per cent on beam loss due to residual gas pressure, then the average pressure in the line should be no worse than 3×10^{-7} torr.

Summary

The total number of optics components required to complete three experimental stations using three achromatic bends is summarized in Table XX. Another high frequency buncher could be used as required near the experimental set-up to provide more flexibility in the longitudinal beam characteristics.

Table XX. Summary of optics components required to outfit HEBT to supply three experimental stations.

Element	Number required
AECL L1 quads	36
AECL L2 quads	2
Q85A quads	6
Q85B quads	1
Trim quads	6
AECL x–y steerers	19
Dipoles $\rho = 100$ cm, $\theta = 22.5°$	6
Low-β buncher	1
High-β buncher	1

ISAC CONTROLS

Detailed design and implementation of additional sections for the ISAC control system proceeded smoothly and the following major milestones were achieved:

- April: Vacuum, optics and diagnostics control for the low energy beam line ILE1 to relocated GPS experiment and LTNO experiment;
- September: Vacuum, optics and diagnostics control for MEBT test #1;
- November: Vacuum, optics and diagnostics control for the low energy beam line ILE2 to β-NMR;
- December: Support for the 100 μA target test.

As of year end, the ISAC control system controls 950 devices, not counting beam line 2A.

Hardware

Two more VME crates were installed. One houses two IOCs for the ILE1 and the ILE2 beam lines, the second houses one IOC which consolidates the PLC supervision for the ITW/IMS/ILE systems. Ethernet based serial interfaces were installed on all IOCs. This allows telnet based console operation of all IOCs from the control room.

For beam line optics, 90 additional device controllers were mounted on high voltage power supplies and added to the CAN-bus network. Special versions were developed to control the Chalk River quadrupole supplies. Problems due to sparks were encountered on the controllers for the electrostatic ion source steering elements. This problem was eventually eliminated by low-pass filtering of the voltage leads at the output of the power supplies.

For beam diagnostics we now use exclusively TRIUMF designed VME modules. An 8-channel bias voltage supply and a harp readout module (VICA) were added to the available module set (more details are given in the Electronics Development section). The ITW harps received the new VICA modules instead of the NIM based 0518 modules. This increased the beam current sensitivity by five orders of magnitude. The VQSX beam current amplifiers were re-configured for higher gain and now allow current measurements down to 10 pA.

The vacuum sub-system controls for the ILE1 and ILE2 beam lines were added to the "target" PLC. Three more PLC breakout cabinets were pre-wired and tested in Trailer Gg and installed on the south mezzanine of the experimental hall and at the DRAGON gas target. The RFQ thermocouple readout system was upgraded to accommodate all 56 thermocouples. The MEBT vacuum control sub-system was upgraded to support the configuration of MEBT test #2 at the beginning of next year.

The last of the four VME PLCs was exchanged with an Ethernet based model in early summer. The three Modbus plus segments were expanded so that each of them can be accessed from both the ion source control room and the ISAC control room.

With the commissioning of the ILE1 beam line, operations moved to the ISAC control room. The control console was set up using two PCs with a combined total of six 21 in. monitors. A four-screen console PC remains in the ion source control room next to the electrical services room for local controls work.

The controls Ethernet section received several hub/repeaters to deal with the increasing number of networked devices.

On the ion source test stand, the control system was expanded for the test of the lithium polarizer. A small PLC was added to the system to accommodate the additional I/O needs. Optics control used standard ISAC CAN-bus modules and diagnostics were temporarily integrated into the existing CAMAC system. In October, the polarizer section was moved from the ion source test stand to the ILE2 beam line. The control sub-system was integrated into ISAC controls.

Software

During this year we were again able to benefit from the high productivity of the EPICS system. The addition of new sub-systems turned into more of a routine exercise and we were able to cope with extremely short commissioning times.

On the operator interface level, the production of many overview screens continued. After a short training period, one member of the operations team started to help in this area and with user interface testing.

The Perl language was introduced to the group and efforts were increased to automate more aspects of the EPICS user interface production. Of the individual device control panels, which contain the display of the device interlock logic, 95% are now automatically generated from specifications contained in a relational database.

The beta testing of the fast channel archiver obtained from LANL was abandoned at the end of the year. It will be replaced by a home-made archiver which is tailored to our needs.

The Web-based fault reporting system was improved and is routinely used, although some additional improvement is desirable.

For the EPICS function block database, CAPFAST schematics were produced for all new sub-systems. Only minor additions were needed at the device and component level.

EPICS device and driver support level was written for:

- the TRIUMF designed 8-channel bias voltage supply;
- the TRIUMF designed VICA harp readout module.

The EPICS infrastructure was upgraded to use the latest EPICS release 3.13.1.

The ladder logic PLC programs were extended to support the new vacuum sub-systems of the ILE1 and ILE2 beam lines and the final MEBT configuration.

Operation

During this year, operation consisted of a mildly chaotic mix of commissioning, upgrading, and "routine" running.

During the 10 μA running period in August, we encountered two crashes each of the beam line 2A PLC and the target PLC. Target PLC crashes are especially severe, as they shut off the heaters of the surface ionization source and lead to thermal shock of the target. The cause of these crashes could not be determined. As a precautionary measure, the target PLC was moved out of the electrical services room onto the experimental hall south mezzanine in early September. In addition, the PLC executives were flash-upgraded to a new revision. Since then, the PLCs have not caused any downtime.

During the same period we also experienced communication lock-ups of the EPICS IOCs approximately once per day. These were traced to an EPICS bug. A patch received from LANL resolved this situation in September.

ISAC DIAGNOSTICS

At times an instrument such as an oscilloscope must be installed close to a signal source but its display is best viewed and controlled from a remote location such as an accelerator operations console. ISAC is controlled using SUN workstations. LABVIEW was installed on one of these and a Tektronix TDS-820 oscilloscope connected to the ISAC Ethernet using a GPIB-Ethernet adapter box. The settings of the oscilloscope could be altered from a PC and the display viewed there via X-Windows and an Ethernet connection. Control from the computer may be simpler than from the device itself since LABVIEW permits a knob or button to be placed on the PC to operate any controllable function of the instrument whereas the oscilloscope may have no room for such knobs and instead uses treed menu screens. The operator-instrument interface may thus be customized. The back-end processor of the TDS 820 limited the refresh rate of the PC to 7 times per second, but this proved to be quite acceptable. In principle any device with a GPIB output may be operated in this way.

A fast Faraday cup has been built at TRIUMF based on a model from INFN-Legnaro, Italy. One difference is that the field defining grid at the entrance may be held at a potential different from ground. Another difference is the use of an SMA connector with ceramic insulation between the current collector and the case. It was calculated that the standard Teflon insulation would restrict the beam power to 4.5 W. The cable between the monitor and the vacuum feedthrough will be the new thermal limiter but it is more easily altered. The cup has operated in a location right at the exit of the RFQ but the mixture of accelerated ions, unaccelerated ions, stray charges and rf pickup made it difficult to check the design. More measurements will be made in a downstream location with a cleaner beam following collimators and magnets.

Previous measurements of the reproducibility in position of scanning wires driven by stepping motors had shown excellent reproducibility, ± 5 μm, under the same conditions of motion, but had also shown a shift in apparent position when the scanning speed or rate of acceleration were altered. Measurements were made, changing the velocity by small amounts and by replacing the scanning blades with a mask cut with several

slots. The results implied that the initial impulse imparted by the stepping motor initiated a vibration; the amplitude and phase of the vibration at the central measuring point depended on the acceleration and speed. It had been the practice to operate stepping motors under constant acceleration or deceleration, i.e. with either a constant force or no force at all. The oscillation amplitude was much reduced by replacing this algorithm with one that increased or decreased the forces smoothly.

A used NEC-FS6 foil changing mechanism has been refurbished, ready for installation in MEBT. Amorphous carbon foils 3 to 7 μg/cm^2, made by vacuum deposition, have been attached successfully to frames. We believe, from the literature, that the foils should be relaxed to extend their working life, i.e. the working surface area of the carbon should be larger than the apertures in the frames in order to accommodate shrinkage under bombardment. The best method to do this is still being investigated. The literature implies that the extension in lifetime seen in foils manufactured by other methods, such as cracking ethylene, is relatively small for the very thin foils used in MEBT and so any such development will await operating experience.

The bunch repetition rate in ISAC-I is 11.8 MHz or 1.2×10^7 ion bunches per second. The flux of some radioactive isotopes is expected to have a similar magnitude. We were interested in how the ions, randomly produced, may be distributed among the bunches. The classic Schottky approach assumes a Poisson distribution in the number of charges in each of a series of time intervals. The length of the time intervals is chosen so that this assumption is valid. The problem for arbitrary or fixed time intervals was re-approached using the binomial theory. We found that the Schottky and binomial approaches agree until there are fewer than 100 bunches in the time interval being considered; the discrepancy increases from 0.5% below this point. The Poisson distribution is a good approximation for a large number of buckets and particles; a high intensity beam in a small number of buckets is better approximated by a normal distribution. We also computed the probability that a bunch may contain more than one ion.

ISAC-II ACCELERATOR

Introduction

Work continued on the ISAC-II accelerator proposal. The ISAC facility now under construction will provide ions of mass $A \leq 30$ up to energies of 1.5 MeV/u. In the ISAC-II facility, the accepted mass range is extended up to 150 and the final energy is increased above the Coulomb barrier ($E \sim 6.5$ MeV/u).

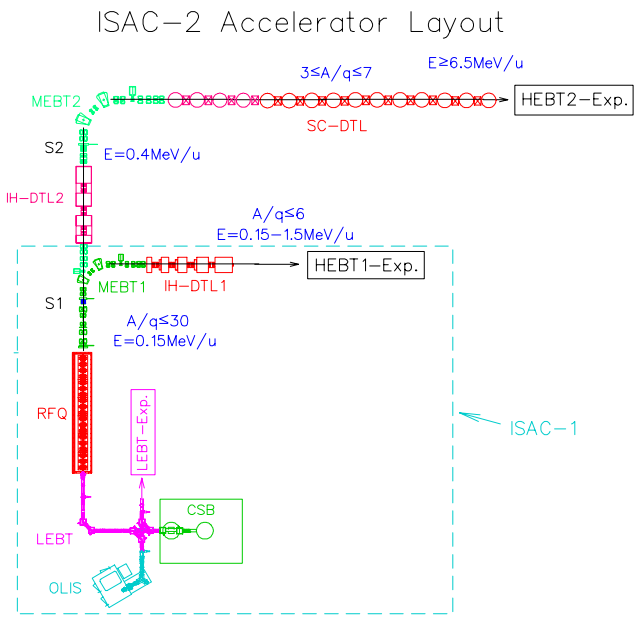

Fig. 154. The ISAC-II linear accelerator complex.

A schematic of the proposed ISAC-II linear accelerator complex is shown in Fig. 154.

To minimize the total acceleration voltage required, the optimum stripping energy for masses of $A \leq 150$ and for $E_{\rm final} = 6.5$ MeV/u is ~400 keV/u. A DTL will be placed downstream of the existing MEBT bender after a short matching section. A room-temperature interdigital H-mode (IH) structure operating in cw mode will be used to accelerate the ions of $A \leq 30$ from $0.15 - 0.4$ MeV/u.

The beam is then stripped and the ion charge selected in a 90° bend (MEBT-2) section to a line parallel to the ISAC-I DTL line. Ions of mass-to-charge ratio $3 \leq A/q \leq 7$ with associated stripping efficiencies varying from 50% for the lightest ions to 15% for $A = 150$ are matched into a superconducting DTL on this line and accelerated to at least 6.5 MeV/u and then transported to the experimental stations. A summary of the linac specifications is shown in Table XXI.

Table XXI. Summary of ISAC-II linac specifications.

Device	$E_{\rm in}$ (MeV/u)	$E_{\rm out}$ (MeV/u)	A/q	$\Delta V_{\rm max}$ (MV)
CSB	–	0.002	≤ 30	0.06
RFQ1	0.002	0.15	≤ 30	4.44
IH-DTL2	0.150	0.40	≤ 30	7.50
strip				
SC-DTL	0.40	6.5	$3 \rightarrow 7$	42.7

Pre-Stripper Linac

The IH linac structure offers very high shunt impedance values making cw operation at room temperature possible. The structure is used in the ISAC

DTL1 variable energy linac design. In this case the application is for a fixed final velocity, so long tanks each containing many drift tubes are used to achieve the highest acceleration efficiency. Magnetic quadrupoles are installed both in tanks and between tanks to provide periodic transverse focusing. The small longitudinal and transverse emittances from the RFQ ($\epsilon_z = 0.3\,\pi$ keV/u ns and $\beta\epsilon_{x,y} = 0.1\,\pi$ mm mrad) allow a frequency of 70 MHz, double that of the RFQ frequency, reducing the size of the DTL tanks and improving the shunt impedance. The shunt impedance for the structure is estimated to be ∼300 MΩ. In a cw DTL the dissipated power is a more limiting factor than the peak surface field in establishing the operating gradient. A power dissipation of 20 kW/m can be safely cooled, requiring an average effective gradient $\overline{E_oT} \leq$ 2.4 MV/m.

In order to reduce the demands on the rf amplifier the DTL is divided into two tanks each with one quadrupole triplet inside, roughly midway down the tank, and one quadrupole triplet between tanks. Each triplet requires ∼65 cm with gradients up to 60 T/m. A diagnostic box will also be added to the intertank region. The total length of the linac is 5.8 m. The beam dynamics utilizes the method developed at GSI where a short −60° section is used after each magnet system for rebunching followed by an accelerating section at a synchronous phase of 0°. The acceptance of the linac is $\epsilon_z = 3.6\ \pi$ keV/u ns and $\beta\epsilon_{x,y} = 0.8\ \pi$ mm mrad.

Table XXII. Gross specifications of the pre-stripper DTL.

Parameter	Value
Initial energy	150 keV/u
Final energy	400 keV/u
A/q	≤ 30
$V_{\rm eff}$	7.5 MV
RF frequency	70 MHz
Type	IH room temperature
Duty cycle	cw
Length	5.8 m
Triplet length	70 cm
Transmission	100%
Emittance growth	< 10%

Table XXIII. Specifications for each tank of the pre-stripper DTL.

Parameter	Tank 1	Tank 2
Energy range	150–250 keV/u	250–400 keV/u
A/q	30	30
$V_{\rm eff}$	3.0 MV	4.5 MV
No. of cells	13, 21	21, 20
$E_{\rm g}$ (MV/m)	2.7	2.7
Length (m)	2.2	3.0
Power (kW)	30	45

With the expected beams from the RFQ, the emittance increase during acceleration is calculated to be less than 5%.

A summary of the gross specifications for the linac is presented in Table XXII and the specifications for each tank are given in Table XXIII. A schematic rendering of the DTL and associated beam envelopes is shown in Fig. 155.

Post-Stripper Linac

The gross specifications of the post-stripper linac are shown in Table XXIV.

A two-gap quarter wave structure is chosen for ISAC-II because of its high velocity acceptance and inherent mechanical stability. The former is useful to accelerate the wide range of ions ($3 \leq A/q \leq 7$) efficiently with a minimum of cavity types and the latter is essential to produce high accelerating gradients. We chose a common linac geometry (INFN-Legnaro, JAERI-Tokai) having four resonators in a cylindrical cryostat with room temperature quadrupoles between cryostats.

Table XXIV. Gross specifications of post-stripper linac.

Parameter	Value
Initial energy	400 keV/u
Final energy ($A/q = 7$)	6.5 MeV/u
Final energy ($A/q = 3$)	15 MeV/u
A/q	$3 \leq A/q \leq 7$
$V_{\rm eff}$	42.7 MV
Duty cycle	cw

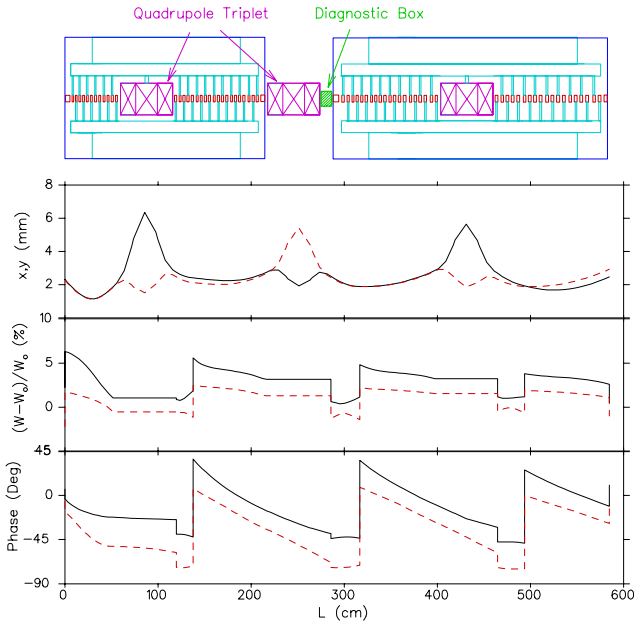

Fig. 155. The pre-stripper IH-linac for ISAC-II and associated beam envelopes.

A cavity is identified by the ion velocity, β_o, required to traverse the distance between gap centres in half an rf oscillation. The distance between gaps is then $\beta_o\lambda/2$ where λ is the rf wavelength. The height of the cavity is $\lambda/4$. Legnaro has reduced the design overhead required between different β_o values by maintaining a constant outer cavity diameter and changing the cavity frequency to alter β_o. Based on the same design principle, three cavity sizes, corresponding to low-, mid- and high-β_o cavities respectively, have been adopted for ISAC-II.

Overall acceleration efficiency plus practical concerns are responsible for the choice of cavity geometries. Firstly, any one cryostat will be outfitted with four identical resonators so the number of cavities of each type will be a multiple of four. A first stage of installation by 2003 will consist of five cryostats loaded with twenty cavities delivering an effective voltage of ∼20 MV to a beam with an initial velocity of 5.6% (1.5 MeV/u). It was decided that in order to limit the early design work, this stage should consist of only mid-β_o cavities designed for $\beta_o = 7.2\%$. The low- and high-β_o values were chosen to optimize the acceleration efficiencies over the whole A/q range. Mass-to-charge ratios from 3–10 were considered; the higher values may be possible direct from the charge state booster (CSB) without stripping. In summary, the chosen cavity geometries correspond to particle velocities of 4.2%, 7.2% and 10.5% the speed of light with cavity quantities of 8, 20 and 20 for a total of 48 cavities. In the low-β_o section a gradient of 5 MV/m is assumed, while 6 MV/m is assumed elsewhere. The acceleration efficiency over the whole acceleration range is shown in Fig. 156(a,b,c) for various A/q values with final efficiency plotted in Fig. 156(d).

A minimum total efficiency of more than 83% is expected for the ISAC superconducting linac. To reach $V_{\rm eff} = 42.7$ MV with an integrated time constant of 82% and an average synchronous phase of $-25°$ requires a voltage of 57.5 MV with roughly 14.4 MV and 43.1 MV from the low- and high-β_o sections respectively.

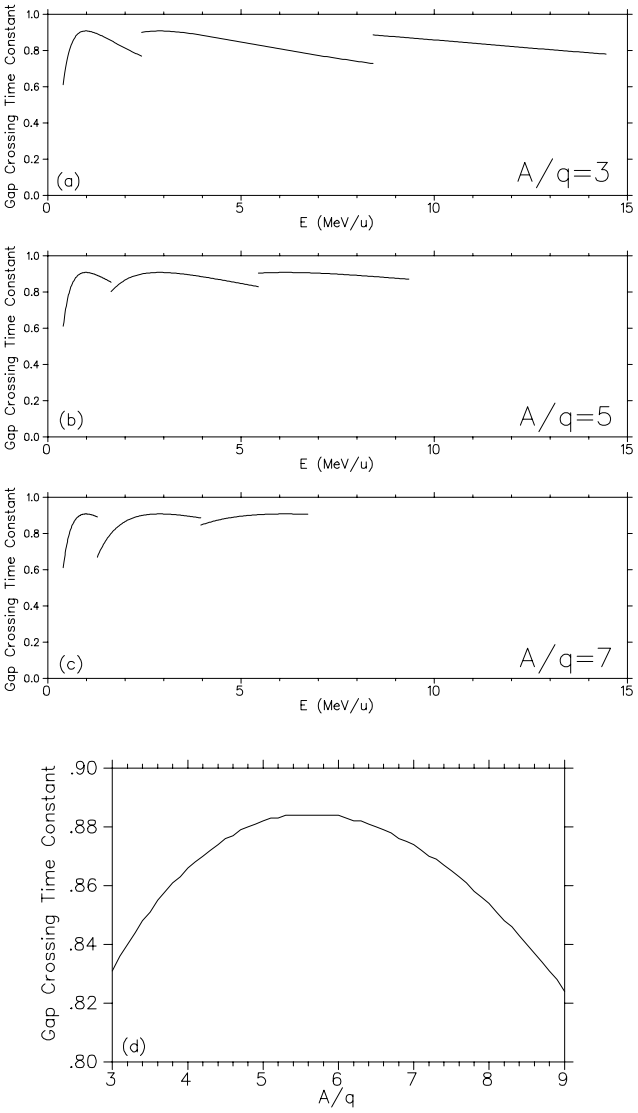

Fig. 156. The acceleration efficiency as a function of particle velocity for various mass-to-charge ratios (a,b,c) using an optimized three β_o accelerating scheme. In (d) the total acceleration efficiency is plotted as a function of A/q.

Cavity Dimensions

Once the design β_o is established the cavity dimensions are set by the rf frequency choice. A lower frequency increases the cavity length, hence reduces the required number of cavities, but requires a longer inner conductor where mechanical oscillations may be problematic. In Table XXV the cell structure for each cavity type is given assuming rf frequencies of 70, 105 and 140 MHz, the $6^{\rm th}$, $9^{\rm th}$ and $12^{\rm th}$ harmonics of the bunch frequency, for the low-, mid- and high-β_o linac sections respectively.

Table XXV. Specifications for the three cavity types. The accelerating voltage assumes a gradient of 5 MV/m.

Parameter	Low-β_o	Mid-β_o	High-β_o
No. of cells	2	2	2
β_o (%)	4.2	7.2	10.6
$f_{\rm rf}$ (MHz)	70	105	140
λ (cm)	428	285	214
$\beta_o\lambda/2$ (cm)	9.0	10.3	11.3
Cavity inner dia. (cm)	18	18	18
Cavity height (cm)	107	71.3	53.5
$E_{\rm g}$ (MV/m)	5	6	6
$V_{\rm acc}T$/cav (MV)	0.85	1.0	1.0

The lower frequency is chosen to match the bucket size of IH-DTL2 taking into account the opposing effects of the reduced relative longitudinal emittance with acceleration and the increase in the longitudinal emittance due to energy straggling in the stripping foil. The rf frequency can be increased with ion energy as the relative longitudinal emittance is reduced through acceleration. The three cavity diameters are identical at 18 cm while the cavity heights vary with frequency. This gives a fixed outer cavity diameter of 20.5 cm, hence a common cryostat diameter for all sections of about 1 m.

Recent developments at Legnaro have shown that cavities of bulk niobium, or with niobium films sputtered on a copper substrate, can deliver effective gradients consistently above 5 MV/m and in some cases as high as 8 MV/m with cooling loads of 7 W at 4 K. The ISAC-II design is based on effective gradients of 6 MV/m in the mid- and high-β_o sections and 5 MV in the low-β_o section. To allow for future developments the beam optics is based on gradients as high as 10 MV/m.

We opt for 8 low-β cavities (2 cryostats), 20 mid-β cavities (5 cryostats) and 20 high-β cavities (5 cryostats) for an effective voltage of 47 MV. The actual acceleration is normalized by the average synchronous phase; a synchronous phase of $-25°$ results in the required voltage gain of ∼43 MV.

Linac Structure

Longitudinal focusing will be achieved by operating the cavities at a negative synchronous phase between –30 to –20°. This produces a net transverse defocusing due to the transverse fields near the entrance and exit of the acceleration gaps. Transverse stability will be maintained by periodic focusing between cryostats. Due to the strength of the accelerating fields and hence the rf defocusing, quadrupole triplets or doublets between each cryostat will be used to refocus the beam into the next cryostat. Periodic triplets have the advantage of keeping the beam small in the accelerating sections but doublets are less sensitive to tuning errors. The transverse focusing is still being optimized.

A short diagnostic box will be included in each inter-cryostat region. Even with a triplet, all cryostat accelerating gradients are limited to 5 MV/m and 7.5 MV/m in the first two cryostats due to the large relative rf defocusing for the low velocity lighter ions. The lattice allows a gradient of 10 MV/m in the remainder of the linac. A summary of the specifications for the post-stripper linac is given in Table XXVI.

Table XXVI. Specifications for each section of the post-stripper superconducting DTL.

Parameter	SC-DTL1	SC-DTL2	SC-DTL3
E (A/q=7)	0.4–1.3 MeV/u	1.3–4.0	4.0–6.6
E (A/q=3)	0.4–2.4 MeV/u	2.4–8.3	8.3–14.6
A/q	3–7	3–7	3–7
β_o	4.2	7.2	10.5
f (MHz)	70	105	140
$N_{\rm cav}$	8	20	20
$N_{\rm cryo}$	2	5	5
$E_{\rm g}$ (MV/m)	5	6	6
Length (m)	2.6	8	8

Beam Simulations

Beams of initial emittance $\beta\epsilon_{x,y} = 0.2\ \pi$ mm mrad and $1.6\ \pi$ keV/u ns for $A/q = 3$ and $A/q = 7$ were simulated in the linac code LANA using a triplet every cryostat and a gradient of 5 MV/m. Growth in the transverse and longitudinal emittance was less than 5%. The longitudinal acceptance in both cases was $50\ \pi$ keV ns; 30 times larger than the design input beam. The transverse envelopes and beam energy for the two cases are shown in Fig. 157.

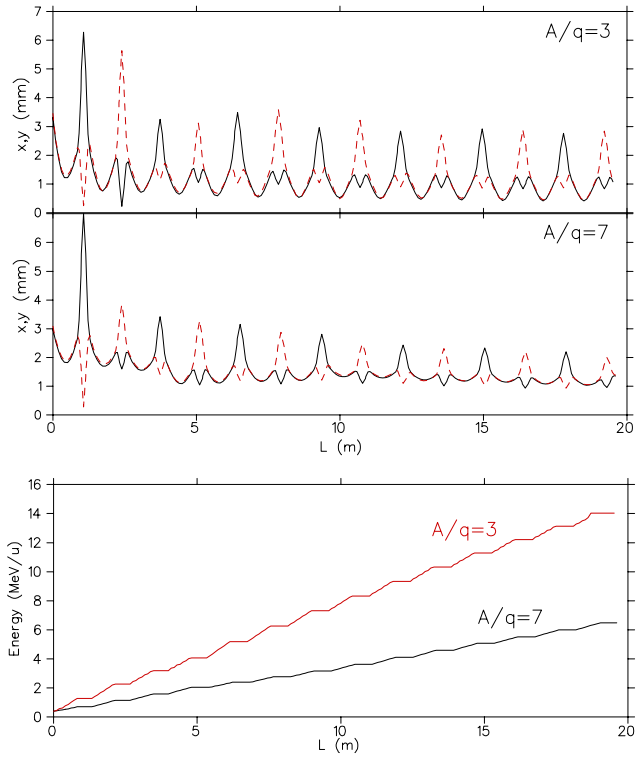

Fig. 157. Beam envelopes and beam energy for the ISAC-II post-stripper linac for design particles of A/q of 3 and 7.

ISAC PLANNING

This year the Planning group was involved in scheduling, coordinating and expediting several projects for ISAC.

Various PERTs were prepared and updated regularly with personnel estimates and analysis to identify critical areas and resolve any problems. The highest priority was assigned to: the construction of two new target modules; to install and test a 100 μA target by December; to complete a hot cell, the remote controls of the target hall crane and the air zoning systems by October; and the β-NMR (stage I) tests with RIB by December 6. On the accelerators, the goals included: test the RFQ at 150 keV/u (August); MEBT tests (Test #1 in August and Test #2 in February, 2000); and design of the DTL and HEBT components. Activities were coordinated and expedited, and the above goals were achieved on schedule.

Progress on PERTed activities is described elsewhere in this report under the respective principal group. However, following is a summary of projects along with the major milestones achieved.

Target Areas and Hot Cells

Main work included design, construction and assembly of two new target modules with improved design, manufacturing and servicing procedures, easy handling, and added provisions for an ECR source. One new target module was assembled with a high power target (December 6–16), and the target was tested successfully on December 17 at 100 μA. In preparation for this, BL2A was commissioned at 100 μA with no target on December 10, and extensive work was done to upgrade target area services, interlocks and controls. Other work included activities on hot cells (manipulators, table, lifting system, services, controls, shielding and doors, etc.), and sealing the areas for pressure zoning. The hot cell was completed to allow remote target removal and installation.

RFQ

After installing and testing 7 rings in 1998, the remaining 12 rings were assembled and installed on schedule in July, along with associated rf, services and diagnostic components. The RFQ was tested successfully (with first beam on August 16) at 150 keV/u.

MEBT

Plans were made to test the MEBT in three stages. For Test #1, efforts focused on the design, fabrication and installation of the MEBT components up to DB5. Chalk River quads were used and a stripper was procured from BNL. The MEBT Test #1 with beam was carried out from August–October. It transported the beam through the RFQ and MEBT up to DB5 with an aim to do Test #2 through the whole MEBT in February, 2000. A 35 MHz rebuncher that was also designed, fabricated and tested will be installed for Test #3 along with the DTL tank 1.

Drift Tube Linac (DTL)

Progress on the DTL was delayed due to lack of resources, higher priority on the RFQ, and the MEBT tests. After the RFQ tests, it was determined that the frequency had to be changed from 35 to 35.36 MHz. The DTL triplets were designed, ordered and steel and coils for triplet 1 were received in December. Detailed design of tank 2 with stems and ridges was completed, along with detailed layout of specifications for tanks 3–5, by December, with an aim to place an order for fabrication of all tanks and support cradles by January 14, 2000, and stems and ridges by February, 2000. It was decided to design one large stand to support all 5 DTL tanks and start fabrication in January, 2000.

HEBT

Major jobs included preparing an engineering layout with the HEBT dipoles designed and ordered for delivery in April, 2000, and specifications of the rf devices (11 MHz and 35 MHz bunchers, chopper, etc.).

Low Energy Experiments

Low energy experiments included TRINAT, GPS (lifetime), LTNO, yield station and β-NMR. Extensive effort was spent in planning, coordinating and expediting activities and critical components from the Machine Shop and outside suppliers for the β-NMR and associated LEBT components. The β-NMR was tested slightly ahead of schedule with ^{8}Li beam on December 3.

CONTRACT ADMINISTRATION

In the past year, seven contracts were awarded:

- Sunrise Engineering Limited (of B.C.) built the MEBT 35 MHz rebuncher vacuum tank.
- Sunrise Engineering Limited also built the steel sub-assemblies for, and assembled the eight DRAGON quadrupole magnets. Everson Electric Limited of Pennsylvania provided the excitation coils.
- Brandt Industries Limited of Saskatchewan built the two west target station shield plugs.
- Sicom Industries Limited (of B.C.) built the twelve DTL quadrupole magnet steel sub-assemblies with Danfysik A/S of Denmark providing the excitation coils. TRIUMF will assemble the magnets.
- Filor Industries Limited of Ontario built the four DRAGON electrostatic dipole electrode rough-welded sub-assemblies.

Personnel Resources

In 1999 the personnel effort for ISAC was slightly less than the previous year. In 1999 the average FTE effort per month was 79.25 people and in 1998 the average was 79.97 people (see Fig. 158).

In 1999 the average monthly personnel effort per system (see Fig. 159) was as follows:

Table XXVII. Personnel effort per system.

System	Monthly FTE
Project management & administration	3.96
Beam line 2A	1.02
Target station	5.47
LEBT	9.95
Accelerator	15.50
Science facilities (TRIUMF personnel)	18.11
Infrastructure	11.02
Integration	12.20
Science facilities (non-TRIUMF personnel)	2.02
Total average FTE monthly personnel	79.25

The total personnel effort since the project began is shown in Fig. 160 and Fig. 161. Figure 160 illustrates the total FTE years per project section and Fig. 161 illustrates the total FTE years by type of personnel. The total effort from January 1, 1996 to December 31, 1999 is 262.88 years of work, based on a FTE month of 150 hours.

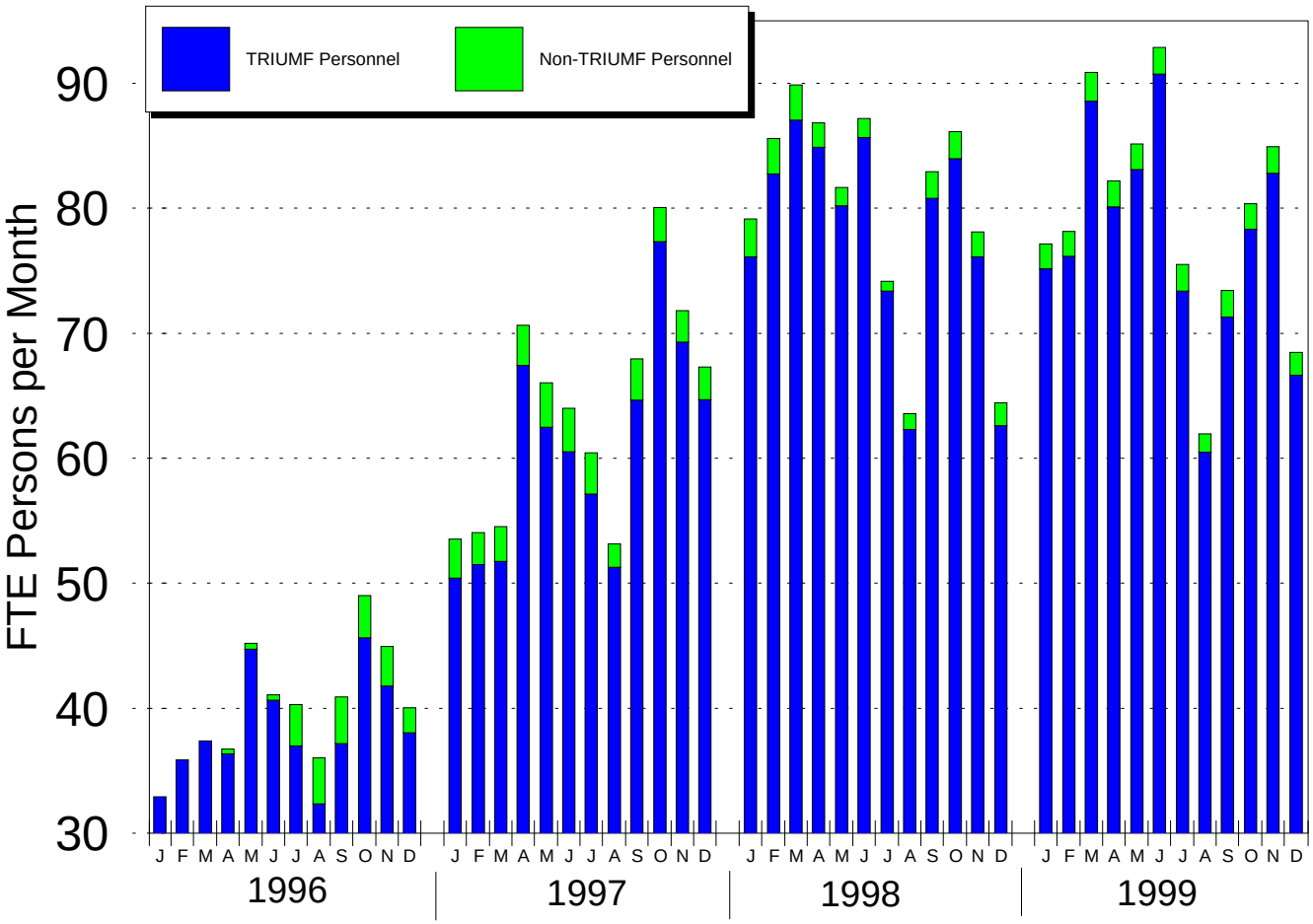

Fig. 158. ISAC project personnel, January 1, 1996 to December 31, 1999.

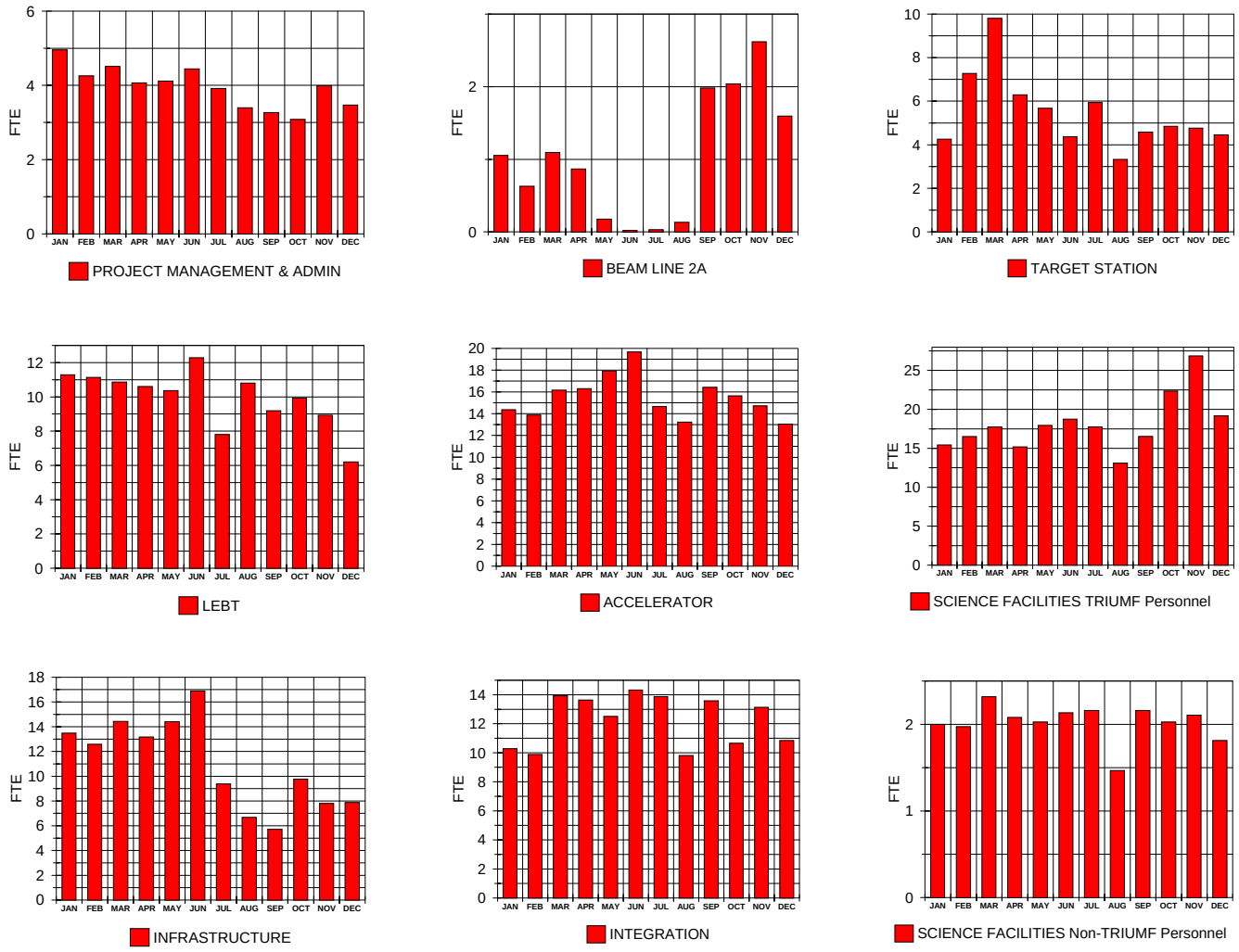

Fig. 159. ISAC project personnel. Monthly FTE people for 1999 (by system).

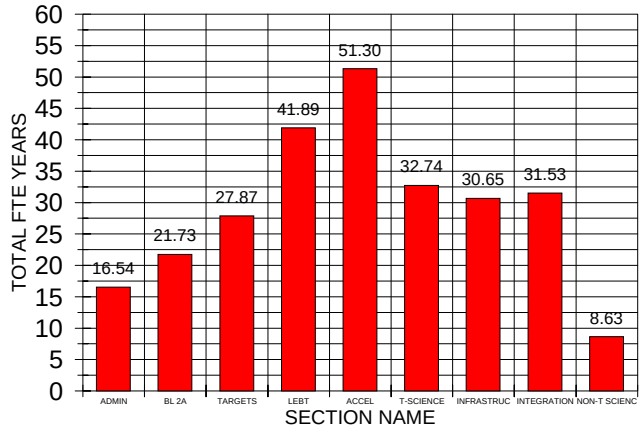

Fig. 160. ISAC project personnel, January 1, 1996 to December 31, 1999 (by section).

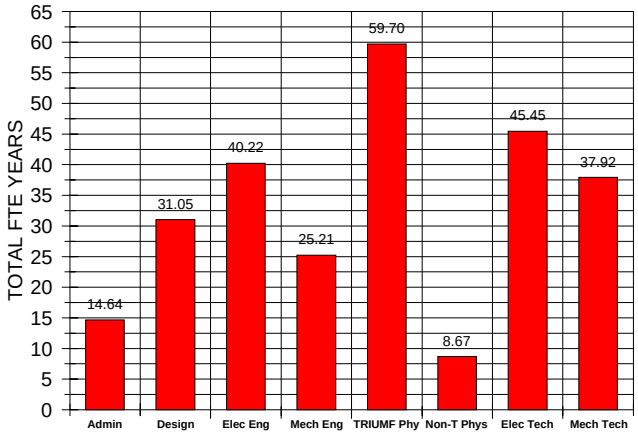

Fig. 161. ISAC project personnel, January 1, 1996 to December 31, 1999 (by personnel type).